# BEAM ANALYZER

## 2. Chromatic and Space Charge Aberrations in Circularly Deflected Electron Beams

N6-ori-71 Task XIX
NR 073 162

TECHNICAL REPORT No. 5-2

ELECTRICAL ENGINEERING RESEARCH LABORATORY
ENGINEERING EXPERIMENT STATION
UNIVERSITY OF ILLINOIS
URBANA, ILLINOIS

# BEAM ANALYZER

## 2. CHROMATIC AND SPACE CHARGE ABERRATIONS IN CIRCULARLY DEFLECTED ELECTRON BEAMS

N6-ori-71 Task XIX
Technical Report No. 5-2
NR 073 162

Date:
September 1952

Sponsored by:

United States Navy
Office of Naval Research

Prepared by:

Heinz Von Foerster

H. M. Von Foerster
Professor

ELECTRON TUBE SECTION
ELECTRICAL ENGINEERING RESEARCH LABORATORY
ENGINEERING EXPERIMENT STATION
UNIVERSITY OF ILLINOIS
URBANA, ILLINOIS

## PREFACE

This report presents an analysis of aberration effects on a circularly deflected electron beam, used as a phase writer system in the beam analyzer built in this laboratory and reported elsewhere*. Since the beam analyzer is supposed to give an accurate picture of the space charge and velocity distribution of the beam under question, it is necessary to investigate possible aberrations which may occur within the analyzing system. Three kinds of aberrations will be discussed in the following chapters.

The first chapter investigates space charge effects in a circularly deflected electron beam. Although the magnitude of these effects may be small in electron beams generally in use, the influence of space charge is not more negligible in beams with very high current density.

Since all deflecting schemes must have a finite extension in space, transit-time effects will cause aberrations which should be properly understood. The second chapter takes phenomena in account which are caused by chromatic aberrations in a deflecting system of finite extension.

Finally, the third chapter makes an attempt to predict deviations of a given density and velocity modulation if the analyzing system for some reason or other cannot be placed at the point of interest. In this case the analysis has to be made at a point on the beam which may be remote from the original point of interest. How to infer from obtained measurements the current and velocity distribution functions at the point of interest will be discussed.

*Contract N6-ori-71 Task XIX, Progress Reports 9 to 14, 18, Technical Report No. 5-1.

## TABLE OF CONTENTS

# CHAPTER I

# SPACE CHARGE EFFECTS IN CIRCULARLY DEFLECTED ELECTRON BEAMS

## SYMBOLS

1) Geometrical Quantities

| | |
|---|---|
| $L$ | Distance from deflection plane along the axis of the deflection cone |
| $L_o$ | a normalized quantity $\beta\lambda/2\pi \sin \alpha$ |
| $R$ | Distance from the axis of the deflection cone |
| $x$ | coordinate perpendicular to the axis of the deflection cone |
| $z$ | coordinate parallel to the axis of the deflection cone |
| $a, b$ | major and minor axis of the elliptical cross section of the apparent beam |
| $r_o, r$ | beam radii before and after deflection |
| $\theta$ | deflection angle in a plane perpendicular to the axis of the deflection cone |
| $\varphi$ | Phase angle |
| $\alpha$ | Deflection angle in a plane going through the axis of the deflection cone |
| $\psi$ | angle between the apparent beam and the generatrix at the point under consideration |
| $\xi, \eta, \zeta$ | reduced coordinates |

2) Electrical Quantities

| | |
|---|---|
| $e$ | charge of the electron |
| $m_o$ | mass of the electron |
| $v_o$ | electron velocity in the direction of the axis of the deflection cone |
| $\beta$ | reduced velocity $v_o/c$ |
| $n_o, n$ | electron density in the beam before and after deflection |
| $\rho_o, \rho$ | space charge density in the beam before and after deflection ($\rho = en$) |
| $\eta$ | surface charge density |
| $I$ | current in amperes |
| $U$ | Voltage in volts |
| $E_R, E_N, E_\theta, E_Z$ | electric field strength in different directions |
| $\lambda$ | free space wavelength |

# 1. INTRODUCTION

The first chapter is concerned with an analysis of space charge effects in a circularly deflected electron beam. The necessity of an analysis of this sort is immediately apparent when the study of pulsed high-power beams or bunches is the center of interest. Three kinds of aberrations will be discussed in the following paragraphs: first, the radial spread of the beam during its path from the deflecting system to its observation plane; second, an angular displacement which allows some electrons to occur at a phase differing from that to which they originally belonged; third, an undesired velocity modulation which may be caused by axial fields, even in continuous uniform circularly deflected beams - an impossibility in a straight cylindrical beam.

The discussion will be opened with an analysis of the geometry involved. Even with the most idealistic assumptions possible, one will soon observe the complexity of the problem. An exact solution cannot therefore be expected, and its attempt would defeat the purpose of this analysis, which looks for a good over-all insight into that problem. This insight should serve as a guide for the design of the experiment. In the course of the discussion several approximations will be made to reduce almost insoluble situations to very workable ones. It is believed that a more accurate study would not reveal more essential features than a rather rough treatment would uncover.

## 2 THE GEOMETRY OF THE CIRCULAR SWEEP

In Progress Reports 9 to 14 a detailed description of the "Phase Writer" element of the beam analyzer has been already given Essentially, the deflecting mechanism consists of two pairs of Lecher wires placed close and perpendicular to each other They fulfill the purpose of producing a rotating electric field which acts on a beam with the same periodicity as that in which the beam is supposed to be modulated (See Fig 1 ) This rotating electric field, perpendicular to the beam under investigation, causes each phase increment $\varphi$ to $\varphi + \Delta\varphi$ of the beam to be deflected in a particular direction $\theta$ and $\theta + \Delta\theta$ and allows a special study of the number or velocity of the electrons pertaining to this section

Since the rotating field produced by the wire system rotates with the same frequency as that in which the beam is modulated, the important relationship can be established

$$\theta = \omega t = \varphi$$

In other words $\theta$ and $\varphi$ are identical in this system

At this point an idealization will be introduced to avoid for the moment complications discussed in Report 13 It will be assumed that this deflecting mechanism can be reduced to a plane, which will be called the "deflection plane" Aberrations caused by the finiteness of the deflection system will be discussed in Chapter II

The deflection of an infinitesimally small section of an electron beam of a finite diameter will take place in such a manner that all electrons of this section will simultaneously obtain a velocity component $v_R$ perpendicular to their initial velocity $v_o$ This will result

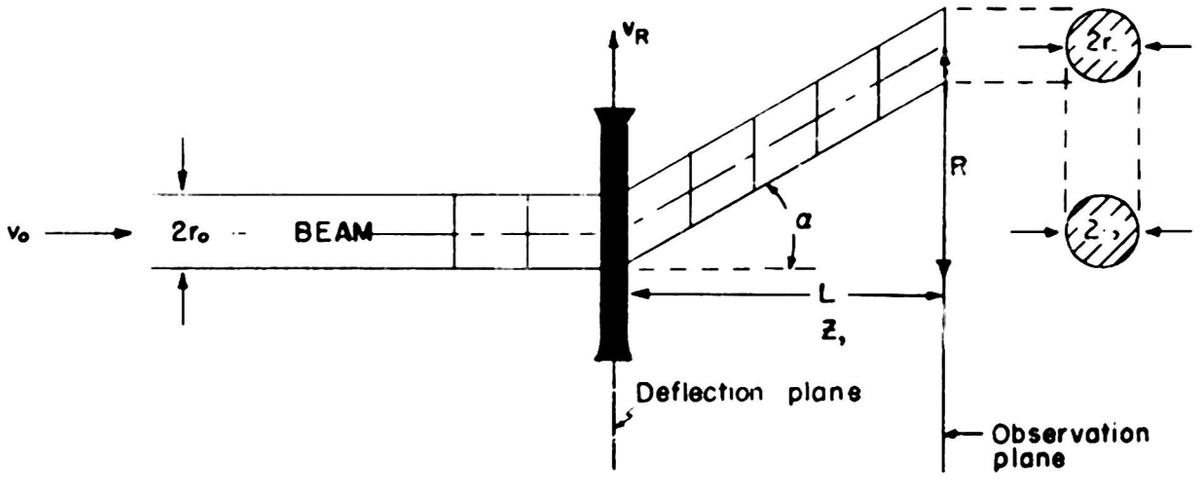


FIGURE 2

in a deflection of the beam of an angle $\alpha(\tan \alpha = v_R/v_o)$, but it will be such that all the electrons (considered in this geometrical section as having no charge) will remain in the same plane which stays parallel to its position in space before and after the deflection.

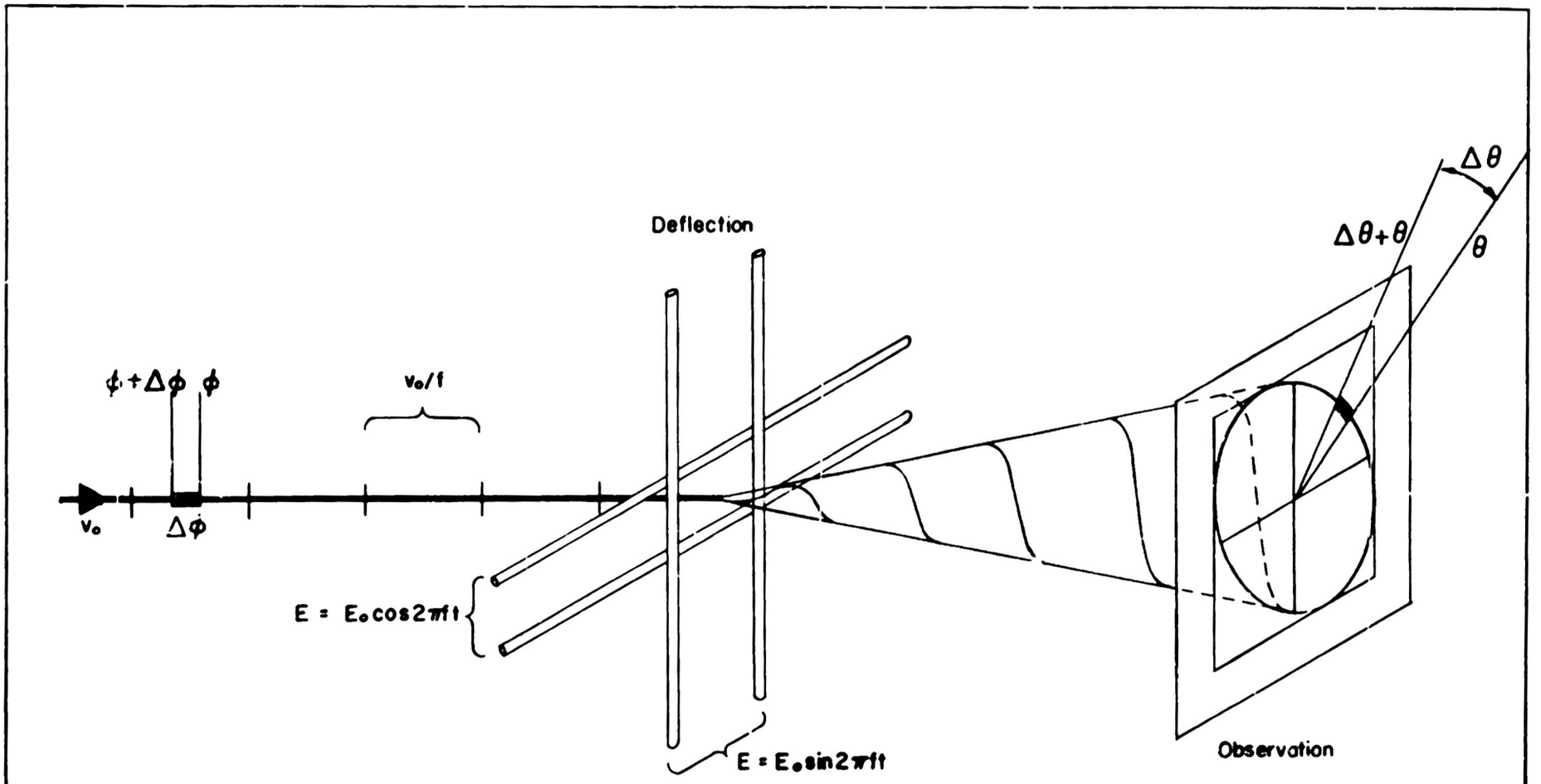
Deflection
$\Delta\theta$
$\Delta\theta+\theta$
$\theta$
$\phi+\Delta\phi$
$\phi$
$v_o/f$
$v_o$
$\Delta\phi$
$E = E_o \cos 2\pi ft$
$E = E_o \sin 2\pi ft$
Observation

FIGURE 1

Since each phase increment $d\theta$ of the beam will be deflected in a different direction $\theta$, each phase increment will travel along a generatrix of a cone with the opening of $2\alpha$. However, if one would make a short exposure of the beam at a particular instant, one would observe the beam in the form of a helix wound around a cone with the opening $2\alpha$. The general equation for this helix can easily be given. With $R = v_R t$, $z = v_o t$, $\omega t = \theta$ (see also Figs. 1 and 2) and $\beta = v_o/c$, one obtains

$$R = \frac{v_R}{\omega}\theta = \frac{v_R \lambda}{2\pi c}\theta = \tan\alpha \frac{v_o \lambda}{2\pi c} = \beta\lambda \frac{\theta}{2\pi}\tan\alpha \tag{1}$$

$$z = \beta\lambda \frac{\theta}{2\pi} \tag{2}$$

Introducing $x = R\cos\theta$, $y = R\sin\theta$, one arrives after simple transformations at the equation for the general helix:

$$y = x \tan 2\pi \frac{z}{\beta\lambda}$$

$$x^2 + y^2 = z^2 \tan^2\alpha \tag{3}$$

and for a particular helix at the instant

$$t_o = \frac{\theta_o}{\omega} = 2\pi \frac{z_o}{\beta\lambda}$$

$$y = x \tan 2\pi \frac{z_o - z}{\beta\lambda}$$

$$x^2 + y^2 = (z - z_o)^2 \tan^2\alpha \tag{4}$$

This particular helix is shown in Fig. 3. In the xy plane of that figure one sees, of course, an Archimedic spiral following the equation

$$R = \left(\frac{\beta\lambda}{2\pi}\tan\alpha\right)\theta \tag{5}$$

(See Eq. (1).)

In the xz plane that projection is easily obtained by eliminating y in (3)

$$x = \frac{z}{\sqrt{1 + \tan^2 2\pi \frac{z}{\beta\lambda}}} \tan\alpha = z \cos 2\pi \frac{z}{\beta\lambda} \tan\alpha \tag{6}$$

Those helices which appear at particular time instances will be called "the apparent beam". From the foregoing it is clear that the electrons don't travel along such an apparent beam. They travel along a straight path until they hit the target.

Since in later sections some of the geometrical quantities will be used, they may be discussed here. One of those is an angle $\psi$ indicated in Fig. 3. It is the angle of the apparent beam with a generatrix at an arbitrary point of the apparent beam. A local diagram of the neighborhood of such a point is given in Fig. 4.

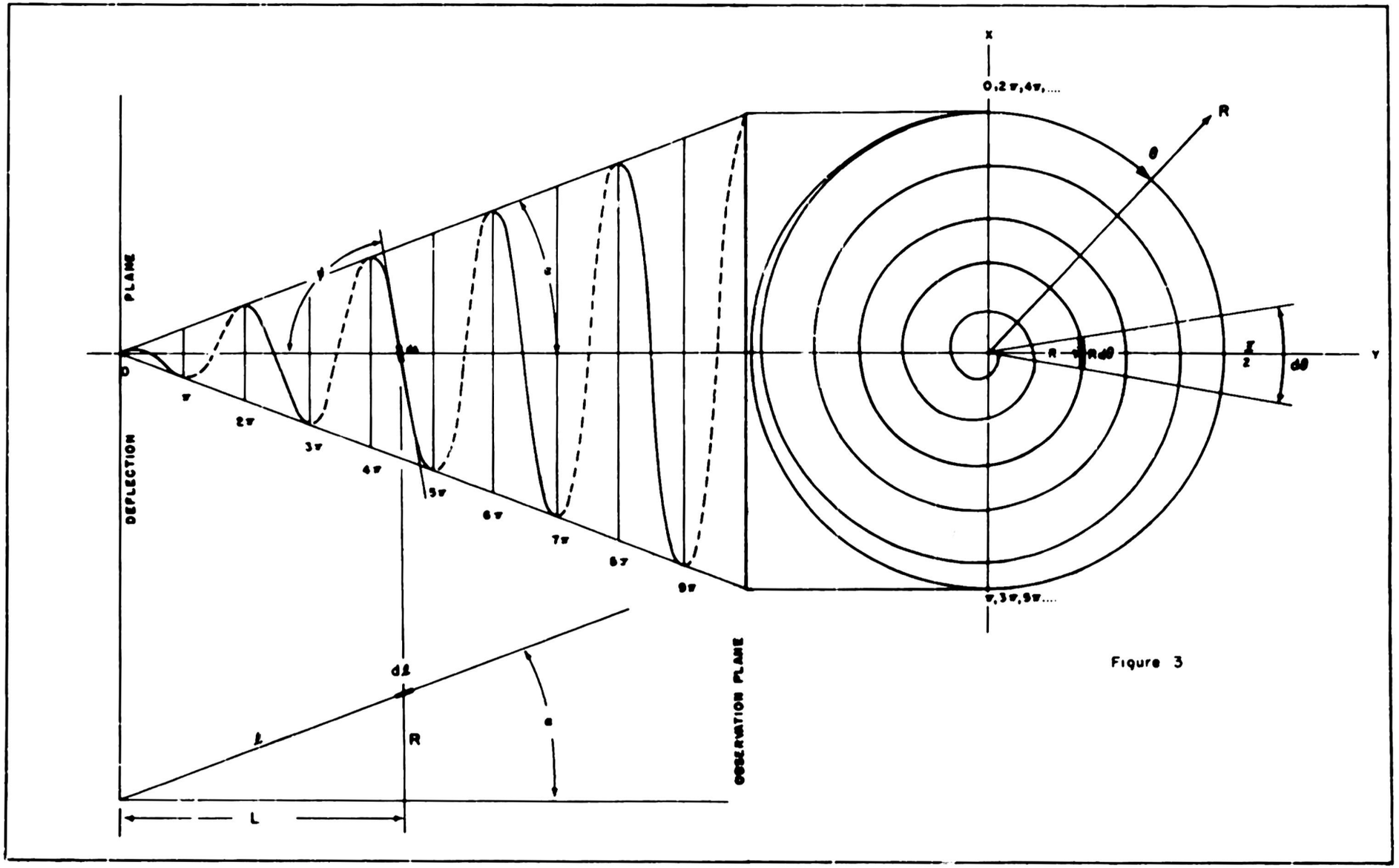
DEFLECTION PLANE
OBSERVATION PLANE
0
π
2π
3π
4π
5π
6π
7π
8π
9π
x
0,2π,4π,....
π,3π,5π....
y
R
θ
dθ
dℓ
ℓ
L

Figure 3

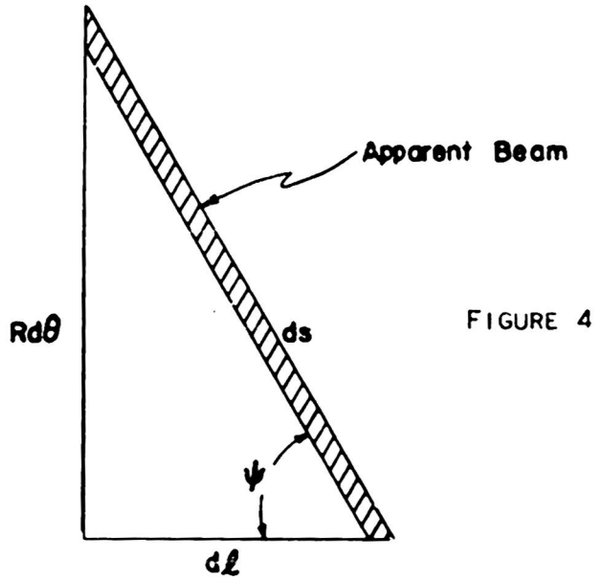


FIGURE 4

In this figure dl denotes an elementary section of the generatrix going through the point in question. ds denotes an elementary length of the apparent beam, and Rdθ the circular section along the base circle of the cone at this point.

Obviously

$$\tan \psi = \frac{R d\theta}{dl}. \tag{7}$$

If the point in question is at a distance L from the deflection plane along the axis of the cone, then

$$l \cos \alpha = L$$

and

$$dl = \frac{1}{\cos \alpha} dL \tag{8}$$

Introducing (8) into (7)

$$\tan \psi = \cos \alpha R \frac{d\theta}{dL} = \cos \alpha R \frac{d\theta}{dL} \frac{dt}{dt}.$$

With the following relations:

$$L = v_o t \qquad \frac{dL}{dt} = v_o \tag{9a}$$

$$\theta = \omega t \qquad \frac{d\theta}{dt} = \omega \tag{9b}$$

$$R = L \tan \alpha \tag{9c}$$

tan $\psi$ can finally be expressed as

$$\tan \psi = 2\pi \frac{L}{\beta\lambda} \sin \alpha \tag{10}$$

From this equation and also from a glimpse at Fig. 3 one can see that $\psi$ increases with increasing distance from the deflection plane. Defining for reasons of convenience

$$L_o = \frac{\beta\lambda}{2\pi \sin \alpha} \tag{11}*$$

$$\tan \psi = L/L_o \tag{12}$$

Thus

$$\cos \psi = \frac{1}{\sqrt{1 + (L/L_o)^2}}$$

$$\sin \psi = \frac{L/L_o}{\sqrt{1 + (L/L_o)^2}} \tag{13}$$

Another geometrical quantity used later will be the elementary length ds of the apparent beam. From Fig. 4 one sees

$$R d\theta = ds \sin \psi \tag{14}$$

and with $R = L \tan \alpha$, (11) and (113) one obtains

$$ds = \beta\lambda \frac{1}{\cos \alpha} \sqrt{1 + (L/L_o)^2} \frac{d\theta}{2\pi} \tag{15}$$

If one is willing to talk about an "apparent beam", it is sensible to ask what the cross section of that apparent beam is. The answer will be given with the aid of Fig. 6.

In the beginning of this section it was shown that an infinitesimally small beam section will travel along a generatrix, but in such a way that the axis of this circular slice remains parallel to itself and to its undeflected direction. Now making a cut perpendicular to the direction of the apparent beam one will no longer see the original slice but the projection of the slice to the plane of the cut. Since the plane of the cut is tilted at an angle $\psi$ against the axis of the slice, and the axis of the slice is tilted against the generatrix at an angle $\alpha$, the cross section of the apparent beam is an ellipse with the two axes

$$a = r \cos \alpha \tag{16}$$

$$b = r \cos \psi \tag{17}$$

where r is the radius of the elementary slice at that point.

*See Figure 5 Nomograph

FIGURE 5

$$L_o/\lambda = \frac{\beta}{2\pi \sin \alpha}$$

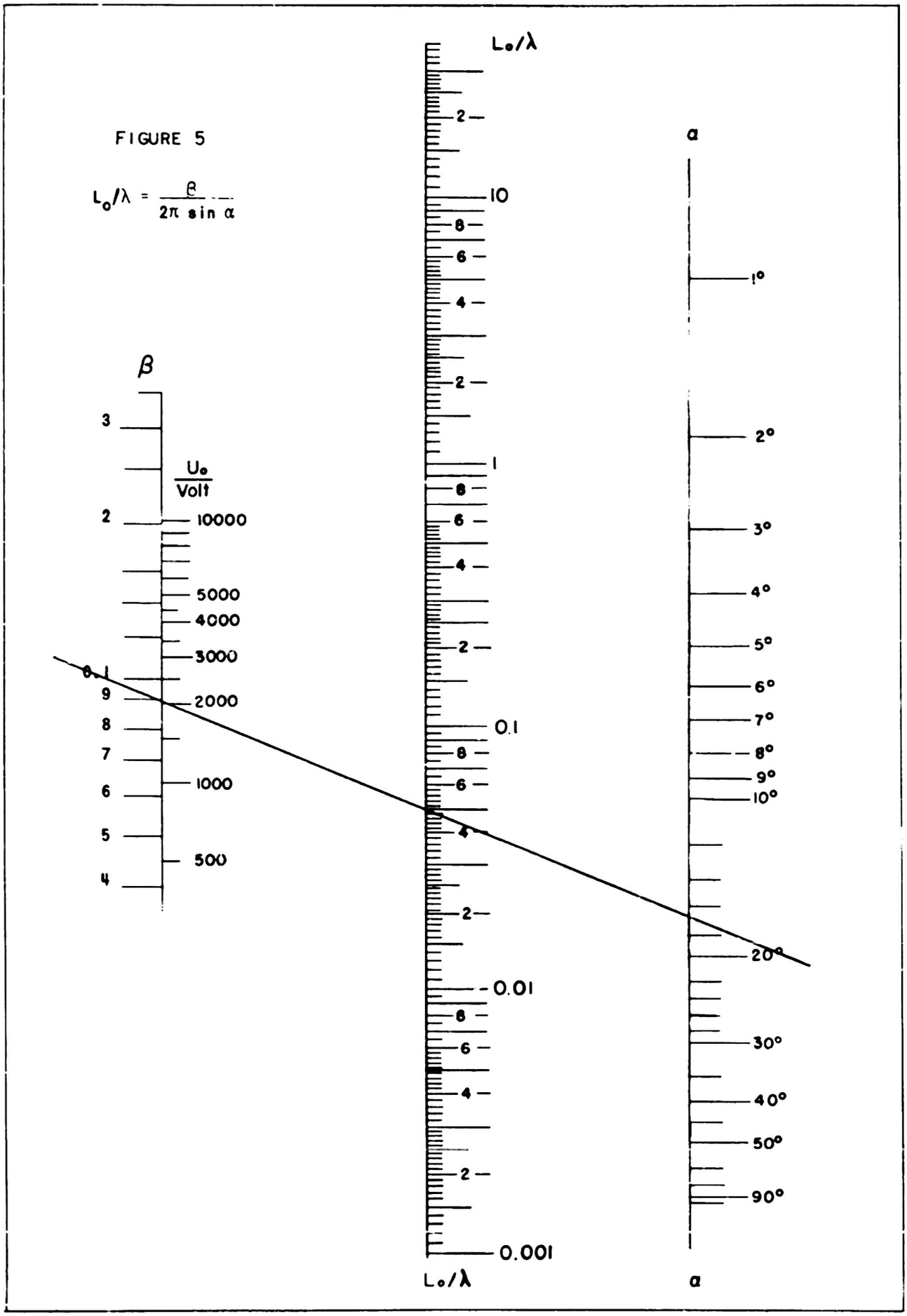

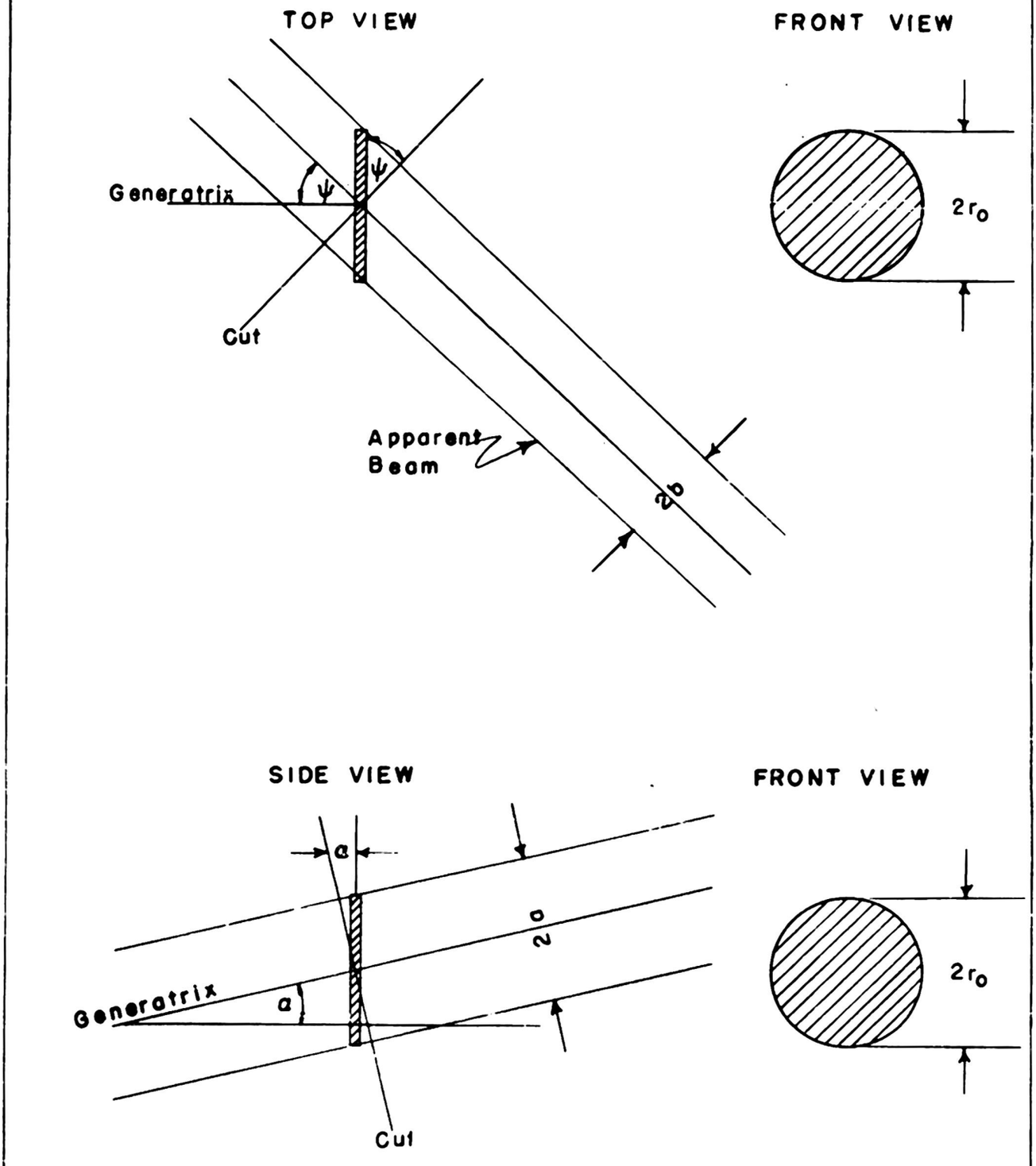
TOP VIEW
FRONT VIEW
Generatrix
Cut
Apparent
Beam
2r_o
SIDE VIEW
FRONT VIEW
Generatrix
Cut
2r_o

FIGURE 6

The first of these two equations shows that one axis, a, remains constant throughout the propagation process, since $\alpha$, the deflection angle, is given by the deflection mechanism. But the second axis, b, is related to the angle $\psi$, which increases with the distance L from the deflection plane. Using Eq. (13) this axis becomes

$$b = \frac{r}{\sqrt{1 + (L/L_o)^2}} \tag{18}$$

This indicates that with increasing length the apparent beam width shrinks to a thin ribbon, moving perpendicular to the plane of the ribbon. This fact will later be a clue to a most startling paradox.

## 3. SPACE CHARGE DENSITY IN A CIRCULARLY DEFLECTED BEAM

In order to compute the mutual forces which act upon tne electrons in the deflected beam it is necessary to know the space charge density on every point along the beam. As it has been pointed out in the preceding section, each phase-increment $\Delta\varphi$ of the undeflected beam will display itself in a corresponding geometrical angle $\Delta\theta$, whereby, by the identity of the modulation frequency of the beam and the sweep frequency of the analyzer, $\Delta\varphi$ and $\Delta\theta$ become identical. This can be used as a guide to compute the space charge density at every point of the deflected beam, for the number of electrons pertaining to a phase increment of the undeflected beam must be the same after they have been swept over the same increment of the geometrical angle.

Call dN the invariant number of electrons in a particular slice of the beam, $n_o$ and n the number of electrons in a $cm^3$ before and after the deflection respectively. Then

$$dN = n_o dV_c = n dV \tag{19}$$

where $dV_o$ and dV are the volume increments of the beam pertaining to the same phase increment before and after the deflection. The volume increment of the undeflected beam is easy to determine:

$$dV_o = \pi r_o^2 dL \tag{20}$$

where $r_o$ is the original beam radius and dL an elementary length along the z axis. The elementary volume of the deflected beam is, of course, its cross section multiplied by its elementary length ds. (See Fig. 3.) Since its cross section is an ellipse with the two axes a and b, this volume becomes

$$dV = \pi\, ab\, ds. \tag{21}$$

With this equation and Eq. (20), the invariance condition (19) becomes

$$dN = n_o \pi\, r_o^2 dL = n \pi\, ab\, ds \tag{22}$$

Expressing dL, ds, a, b in general terms of that geometry, as was done above

$$dL = \beta\lambda \frac{d\theta}{2\pi} \tag{2}$$

$$ds = \beta\lambda \frac{1}{\cos\alpha} \sqrt{1 + (L/L_o)^2}\ \frac{d\theta}{d\pi} \tag{15}$$

$$a = r \cos\alpha \tag{16}$$

$$b = r \Big/ \sqrt{1 + (L/L_o)^2} \tag{18}$$

and inserting these expressions into (22), one obtains the paradoxical result

$$r_o^2 n_o = n r^2. \tag{23}$$

Or, in other words, the electron density of a circularly deflected beam changes precisely as an undeflected cylindrical beam would do.

Assuming for a moment no electrostatic forces, which would blow up the original radius, then r would remain the same and (23) would read

$$n = n_o \qquad (24)$$

In spite of the tremendous spread of the beam due to its conical expansion, the density of the beam is invariant before and after the deflection. The explanation of this phenomenon lies, of course, in the thinning out-process of the beam discussed earlier. This thinning out of the beam exactly makes up for its elongation, and the volume per phase increment and the density remain the same.

## 4. SOLVING POISSON'S EQUATION FOR A SIMPLIFIED GEOMETRY

The amount of aberration of electrons in the beam from their theoretical straight path along a generatrix of the cone can be computed only if the forces which would displace them are known. This would mean solving Poisson's Equation

$$\Delta V = 4\pi\rho \qquad (25)^*$$

for the geometry involved with the notion of the space charge $\rho = en$ from the preceding paragraph. This seems to be an impossible task. It is therefore advisable to make a simplifying change of the geometry without disturbing the physics of the problem too much. In Fig. 7 the geometrical approximation is suggested. Consider the two open ends A and B in 7A bent so that they touch one another and form a complete circle (7B). The forces $E_N$ and $E_R$ exerted on the electrons at the points $P_1$ and $P_2$ will scarcely change, since essentially neighboring electrons will contribute to the fields at points $P_1$ and $P_2$. Furthermore the change in field strength at $P_1$ and $P_2$ will be very small, since this bending action averages out distant forces which may stem from the regions close to A and B. The influence of other cycles of the conical helix will be neglected. Allowing this geometrical simplification, the task remains to solve Poisson's Equation for a space-charge filled toroid with an elliptical cross section. Since this geometry has

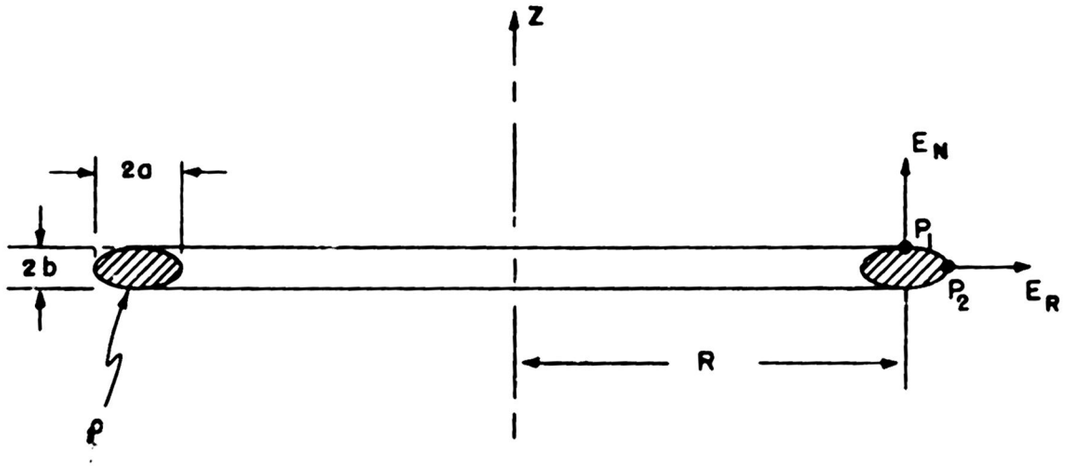


FIGURE 8

cylindrical symmetry, and $\rho$ remains constant along the whole toroid, Poisson's equation reduces to

$$\frac{\partial^2 V}{\partial z^2} + \frac{1}{r}\frac{\partial}{\partial r}\left(r\frac{\partial V}{\partial r}\right) = 4\pi\rho \qquad (26)$$

*Electrostetic System.

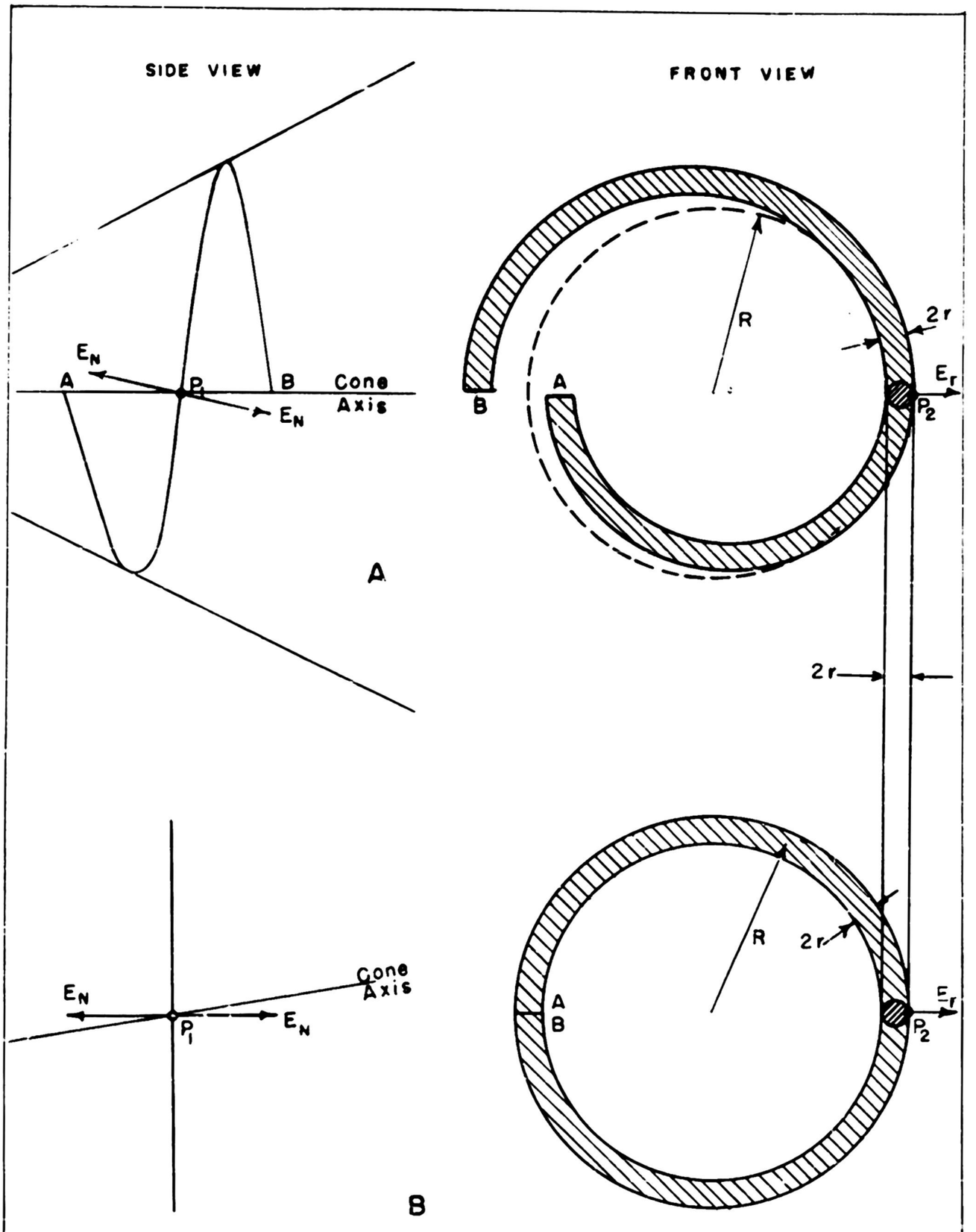
SIDE VIEW
FRONT VIEW
$E_N$
A
$P_1$
B
Cone Axis
$E_N$
A
B
R
2r
$E_r$
$P_2$
2r
A
B
$E_N$
Cone Axis
$E_N$
$P_1$
R
2r
$E_r$
$P_2$
B

FIGURE 7

If one considers the mathematical complications by introducing the boundary conditions of an elliptical toroid, a further geometrical simplification is advisable. Realizing that only the most exposed points $P_1$ and $P_2$ on the surface of that toroid are worth considering and that the beam soon approaches a ribbon-like shape, one will introduce a rather pessimistic picture by changing the elliptical cross-section into a rectangular one (see Fig. 9). This picture is pessimistic in the sense that the surface fields $E_N$ and $E_R$ in the approximated

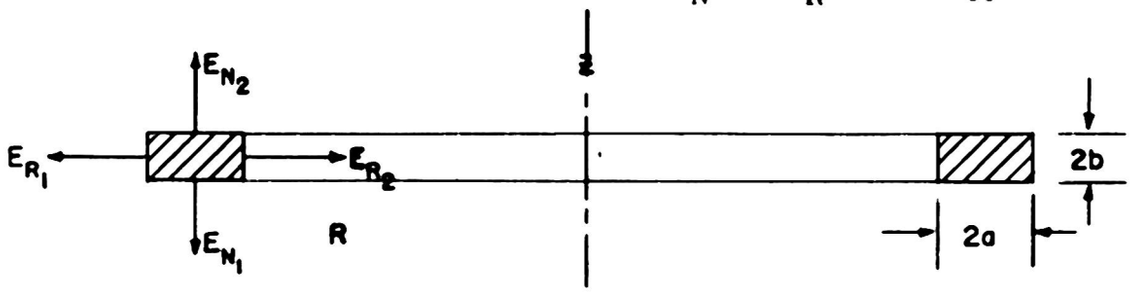


FIGURE 9

picture will turn out to be slightly higher than in the correct one and may therefore give displacement effects which are slightly greater than they actually would be.

The strongest use one can make of the notion of the rapid shrinking process of the beam in the z direction is in treating the rectangular toroid as a ringshaped surface charge. Generally, by passing through such a surface charge $\eta$, the jump of the field in the z direction is given by

$$E_{N_1} - E_{N_2} = 4\pi\eta \tag{27}$$

Since $E_{N_1}$ and $E_{N_2}$ are opposite and equal

$$E_{N_1} + E_{N_2} = 0 \tag{28}$$

the field in the z direction becomes

$$E_N = 2\pi\eta \tag{29}$$

For a thin layer with the space charge $\alpha$ one can express (29) in the form

$$\Delta E_N = 2\pi\rho\Delta z \tag{30}$$

and obtain for the surface field on one side after integration over the minor axis b of the ellipse

$$E_N = 2\pi\rho b \tag{31}$$

From (30) one can obtain immediately an expression for $\frac{\partial^2 V}{\partial z^2}$, for

$$\frac{\partial^2 V}{\partial z^2} = \frac{\partial E_N}{\partial z} = 2\pi\rho \tag{32}$$

Substituting this expression in the Poisson's Eq. (26) one obtains

$$\frac{1}{r}\ \frac{\partial}{\partial r}\left(r\ \frac{\partial V}{\partial r}\right) = 2\pi\rho \tag{33}$$

Since

$$\frac{\partial V}{\partial r} = E_R\ ,$$

the first integral carried out over the proper limits gives

$$\int_{(R-a)E_{R_2}}^{(R+a)E_{R_1}} d(rE_R) = 2\pi\rho \int_{(R-a)}^{(R+a)} r\ dr \tag{34}$$

or, integrated

$$E_{R_1} = \frac{(R-a)}{(R+a)}\ E_{R_2} + 4\pi\rho\ \frac{Ra}{R+a} \tag{35}$$

The field $E_{R_2}$ pointing inwards can be defined by solving Laplace's equation for the center region where no space charge exists:

$$\frac{1}{r}\ \frac{\partial}{\partial r}\ (r\ E_R) = 0 \tag{36}$$

The first integral gives

$$rE_R = \text{constant} \tag{37}$$

where the constant must be zero, since no field can exist at the center of the ring. With

$$E_{R_2} = 0$$

and with Eq. (35) one obtains the radial field $E_R$ pointing outward

$$E_R = 4\pi\rho\ \frac{Ra}{R+a} \tag{38}$$

The results of this section can be summarized in a few words as follows: with three steps of simplification of the geometry of a space charge uniformly distributed over an Archimedic helix with an elliptical cross section, approximate expressions for the electric field strength in the direction of the two axes of the cross section were derived. They are

$$E_N = 2\pi\rho b \tag{31}$$

$$E_R = 4\pi\rho a\ \frac{1}{1+\frac{a}{R}}\ . \tag{39}$$

The three steps of approximation were the following:

a) The helix was cut at the two points opposite the point of consideration and the ends bent to a complete circle.

b) The elliptical cross section was treated as a rectangular one with preservation of the dimension of the axes of the ellipse.

c) The field in the direction of the minor axis was computed as if the minor axis would be much smaller than the major one.

That these crude assumptions give quite good results even at points of the helix where the deviations of a cylindrical beam are almost unobservable (namely close to the deflection plane with a small deflection angle $\alpha$), shows that for $R = a$ and for $\cos \alpha = 1$,

$$E_N = E_R = 2\pi\rho r_o,$$

an expression one obtains by computing the field strength on the surface of an infinitely long cylindrical beam. By increasing the distance from the deflection plane, the approximations become more and more valid.

## 5. RADIAL EXPANSION

After having obtained expressions for the field strength on the surface of the beam in the two axial directions one can immediately obtain expressions for the equation of motion in both directions. First, the expansion in the radial direction will be discussed. Since the major axis a points in the R direction (see Figs 8 and 10), the

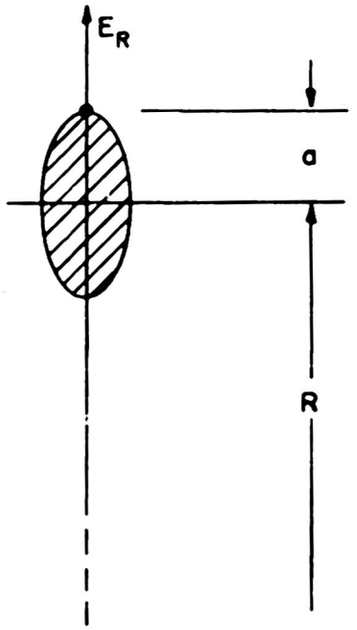


FIGURE 10

equation of motion of the electron on top of the ellipse reads, using Eq. (39) for $E_R$,

$$m \frac{d^2a}{dt^2} = eE_R = 4\pi\rho\, ea \frac{1}{1 + \frac{a}{R}} \tag{40}$$

With

$$a = r \cos \alpha \tag{16}$$

$$\rho = \rho_o \frac{r_o^2}{r^2} \tag{23}$$

$$R = L \tan \alpha \tag{9c}$$

$$L = v_o t \tag{9a}$$

Equation (40) becomes

$$\frac{d^2r}{dL^2} = \frac{2\pi\rho_o e}{mv_o^2} \frac{r_o^2}{r} \cdot \frac{2}{1 + \frac{r}{L} \frac{\cos^2 \alpha}{\sin \alpha}} . \tag{41}$$

Introducing the new variables

$$\eta = r/r_o \qquad \xi = L/L_1 \tag{42}$$

and the constants

$$A = \frac{2\pi\rho_o e}{m_o v_o^2} \tag{43}$$

$$L_1 = r_o \frac{\cos^2 \alpha}{\sin \alpha} \tag{44}$$

the differential equation (40) reduces to

$$\eta'' = \frac{2A}{L_1^2} \cdot \frac{1}{\eta} \cdot \frac{1}{1 + \frac{\eta}{\xi}} \tag{45}$$

An exact solution of this differential equation can only be given with numerical integration. However, a very good approximate solution can immediately be obtained by considering the fact that almost always $\xi >> \eta$. In other words, $\eta/\xi$ can be neglected in comparison with 1 and (45) reduces further to a differential equation of the form

$$\eta'' = K \frac{1}{\eta}$$

Fortunately, this equation is solved in almost all textbooks concerning electron beams*, because it is the equation governing the spread of a cylindrical electron beam. The solution for this particular problem is

$$L = \frac{1}{2\sqrt{A}} \int_0^{\eta} \frac{d\eta}{\sqrt{\ln \eta}} \tag{46}$$

where graphical and nomographical solutions are given elsewhere*. The difference in the usual beam spread formula is that the spread of this helical beam occurs only outward and is about $\sqrt{2}$ times larger than in the cylinder beam case. The reason for the factor $\sqrt{2}$ can easily be found in the fact that in approximating Eq. (45) by neglecting $\eta/\xi$ one always integrates over a $\eta''$ larger than it actualiy would be, if one considered the factor

$$\frac{1}{1 + \frac{\eta}{\xi}} < 1.$$

*See, for example, Spangenberg "Vacuum Tubes", McGraw-Hill, 1948, p. 441.

Since subsequently constant use will be made of the quantity A, a more practical expression will be derived with

$$\rho_o = \frac{I_o}{r_o^2 v_o}$$

$$v_o = \sqrt{\frac{2e}{m_o}} \sqrt{U_o}$$

$$\beta = v_o / v.$$

A becomes

$$A = 1.18 \times 10^{-4} \frac{I_A}{\beta^3} \cdot \frac{1}{r_o^2} \qquad (47)$$

or

$$A = 4.7 \times 10^{-4} \frac{I_{mA}}{U_{KV}^{3/2}} \cdot \frac{1}{r_o^2} \qquad (48)$$

## 6. ANGULAR DISPLACEMENT

More interesting and significant for a device which is built for an analysis of an RF modulated beam than just a little beam spread which would only increase the beam spot and could have been easily anticipated anyway, are aberrations which are caused by the electrostatic field pointing in the direction of the minor axis b of the ellipse - in other words, caused by the field $E_N$, which lies in a plane parallel to the axis of the cone and normal to the helix. Drawing in detail the geometrical situation of the neighborhood of an electron where $E_N$ exerts its

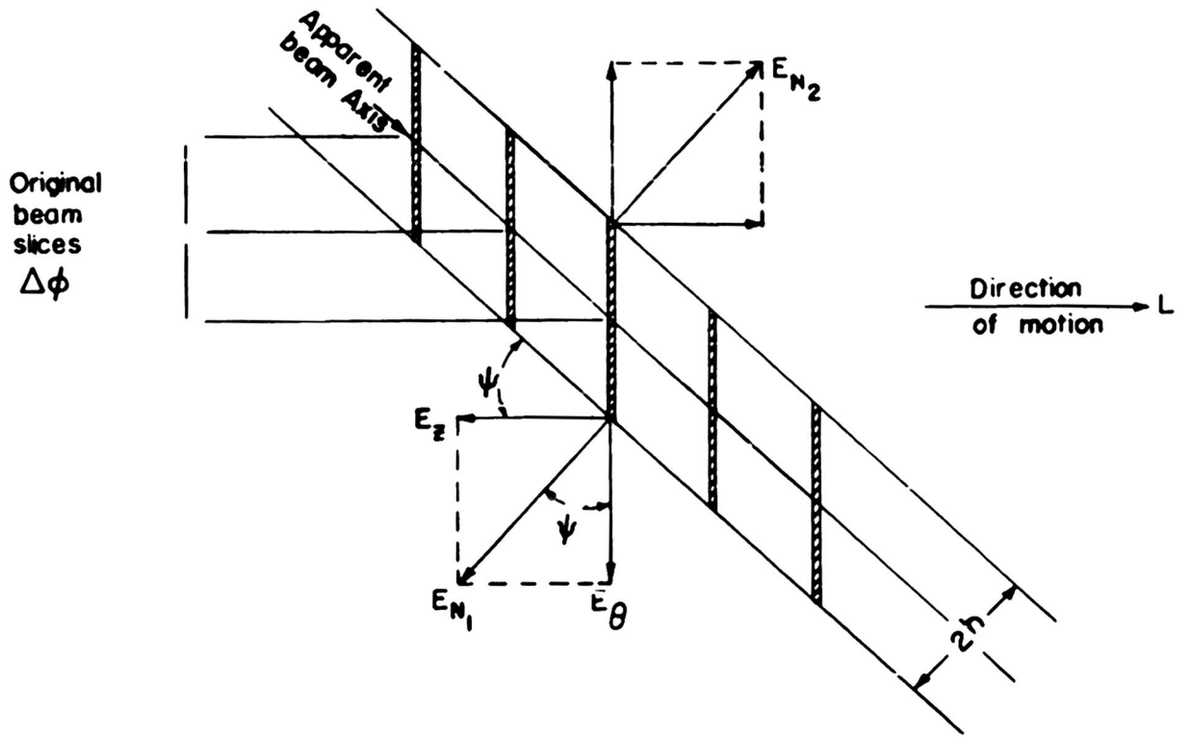


FIGURE 11

force (Fig. 11, see also Figs. 3,4,6), one can immediately recognize two facts:

a) The fields $E_{N_1}$ and $E_{N_2}$ acting on two opposite electrons of the same original beam slice have the tendency to tilt that slice so that it does not preserve its original direction but tries to adjust its axis to the axis of the apparent beam.

b) The field $E_N$ on either side of the apparent beam can be split into two components. The one, $E_\theta$, pushes the electrons out of their original angular location into regions which should be occupied by electrons belonging to this region only, thus causing an angular displacement. The other one, $E_Z$, pushes the electrons in the forward or

backward direction (depending on whether one looks at the front or the rear portion of the apparent beam) thus causing an additional velocity modulation in the direction of the axis of the cone. In this section only the angular displacement will be discussed.

For the field in the tangential direction, $E_\theta$, one obtains with Fig 11

$$E_\theta = E_N \cos \psi. \tag{49}$$

With

$$E_N = 2\pi\rho b \tag{31}$$

$$\rho = \rho_o \frac{r_o^2}{r^2} \tag{23}$$

$$b = r \cos \psi \tag{17}$$

$$\cos \psi = 1/\sqrt{1 + (L/L_o)^2} \tag{13}$$

$$A = \frac{2\pi\rho_o e}{m_o v_o^2} \tag{43}$$

$$L = v_o t \tag{9a}$$

$$E_\theta = \frac{m_o}{e} \frac{d^2 r}{dt^2} \tag{50}$$

Equation (49) becomes

$$\frac{d^2 r}{dL^2} - A \frac{r_o^2}{r} \frac{1}{1 + (L/L_o)^2} \tag{51}$$

Since one is interested in the actual displacement $x = r - r_o$ (see Fig. 12),

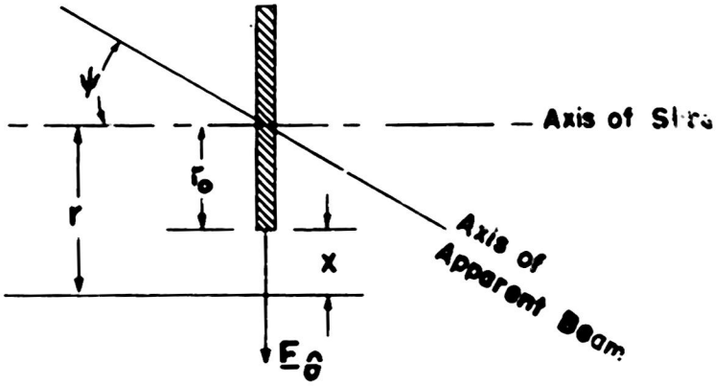


FIGURE 12

new variables will be introduced:

$$\eta = x/r_o$$
$$\xi = L/L_o \tag{52}$$

With these variables in Eq. (51), one obtains

$$\eta'' = AL_o^2 \frac{1}{1+\eta} \cdot \frac{1}{1+\xi^2} \tag{53}$$

This differential equation does not occur in literature and should be solved numerically. But one can immediately find a good approximation of this differential equation for that particular physical problem by remembering that for short distances ($\xi$ not much larger than 1) the displacement $\eta$ will remain about zero, or at least $\eta << 1$. Using a solution for $\eta$ for short distances $\xi$ one can introduce $\eta$ into Eq. (53) and solve for large $\xi$, where $\xi^2 >> 1$. With this program in mind Eq. (53) becomes

$$\eta'' = AL_o^2 \frac{1}{1+\xi^2} \tag{54}$$

Double integration with the limits

$$\text{for} \quad \xi = 0 \quad \begin{cases} \eta = 0 \\ \eta' = 0 \end{cases} \tag{55}$$

gives

$$\eta = AL_o^2 \left[\xi \arctan \xi - \tfrac{1}{2} \ln (1+\xi^2)\right] \tag{56}$$

To correlate the displacement $x = \eta r_o$, expressed in units of length, with the angular displacement $\Delta\theta$, expressed in radians, one has only to introduce the identity

$$x = R\Delta\theta. \tag{57}$$

With

$$R = L \tan \alpha \tag{9c}$$

$$\xi = L/L_o, \quad \eta = x/r_o \tag{52}$$

this becomes

$$\eta = \frac{L_o}{r_o} \xi \, \Delta\theta \tan \alpha \tag{58}$$

Expressing $\eta$ in Eq. (56) in terms of the angular displacement with (58), the displacement angle $\Delta\theta$ becomes

$$\Delta\theta = \frac{AL_o r_o}{\tan \alpha} \left[ \arctan \xi - \frac{\ln(1+\xi^2)}{2\xi} \right] \tag{59}$$

If, for convenience, one defines the function of $\xi$ in the above equation in the following way

$$F(\xi) = \frac{2}{\pi}\left[\arctan \xi - \frac{\ln(1+\xi^2)}{2\xi}\right] \tag{60}$$

the displacement angle $\Delta\theta$ can finally be expressed in the form

$$\Delta\theta = \frac{AL_o r_o}{\tan \alpha} \cdot \frac{\pi}{2} F(\xi) \tag{61}$$

The function $F(\xi)$ is plotted in Fig. 13 As one can see, for $\xi$ approaching infinity, the function approaches the value 1. And furthermore, this asymptotic value is approximately reached quickly for small values of $\xi$. Physically this means that an edge electron belonging to a phase $\theta$ and pushed by the forces of the $E_N$ field will creep into other phases until it reaches a particular phase $\theta \pm \Delta\theta_\infty$ in which it will stay forever $\Delta\theta_\infty$ is given by

$$\Delta\theta_\infty = \frac{AL_o r_o}{\tan \alpha} \cdot \frac{\pi}{2} \tag{62}$$

To express $\Delta\theta_\infty$ in more convenient units, the following relations, already derived, will be used

$$A = 1.18 \times 10^{-4} \frac{I_A}{\beta^3} \cdot \frac{1}{r_o^2} \tag{47}$$

$$L_o = \frac{\beta\lambda}{2\pi \sin \alpha} \tag{11}$$

One thus obtains two equivalent equations for $\Delta\theta_\infty$, where either one can be used at convenience.

$$(\Delta\theta_\infty)_{\text{Radians}} = 2.95 \times 10^{-6} \frac{I_A}{\beta^2} \frac{\alpha}{r_o} \cos \alpha \tag{63}$$

$$\Delta\theta_\infty^o = 0.42 \frac{I_A}{U_{KV}} \frac{\alpha}{r_o} \cos \alpha \tag{64}$$

With these expressions this section is not quite finished, for, as it was pointed out earlier, a better solution for the differential equation (53) could be obtained using the solution for $\eta$ from Eq. (56) as a first order approximation, inserting this result into Eq (53), and integrating again. But by doing that, little would be gained. One also obtains a limiting displacement angle which is defined by

$$\Delta\theta_\infty^* = \frac{AL_o r_o}{\tan \alpha} \tag{65}$$

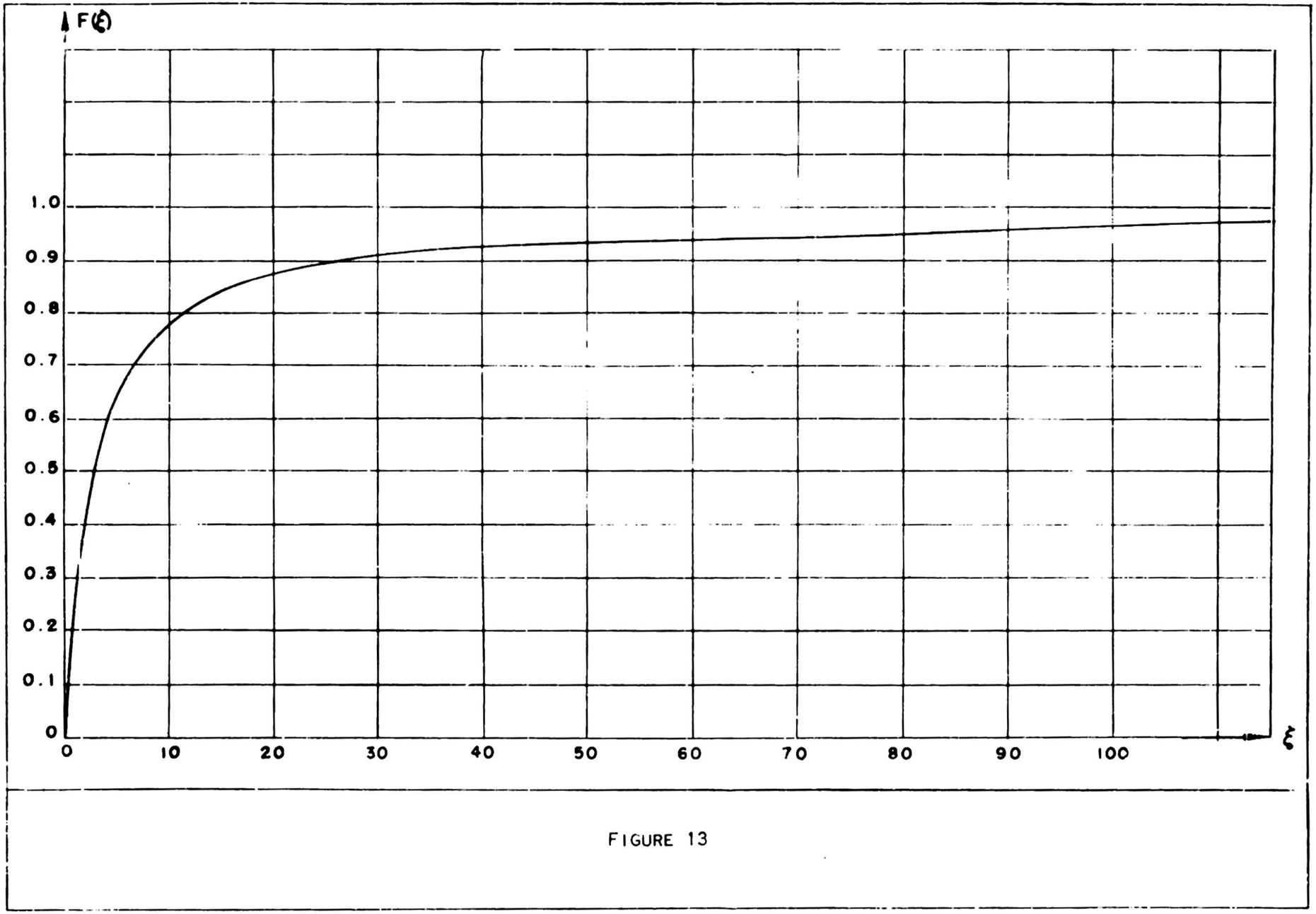


FIGURE 13

This angle is smaller than the one obtained in Eq. (62) by a factor of $2/\pi$. The true angle will probably lie between the two. But, inclined to rely more on pessimistic results, the displacement angle as derived in Eq. (62) or (63) and (64) will be used in further work.

Example:

$$\left.\begin{aligned} I &= 200 \text{ mA} \\ r_o &= 1 \text{ mm} \\ \lambda &= 10 \text{ cm} \\ U_o &= 1.0 \text{ kv} \\ \alpha &= 10^\circ \end{aligned}\right\} \qquad \Delta\theta_\infty^\circ = 8^\circ$$

## 7. AXIAL VELOCITY MODULATION

As it was pointed out in the preceding section, due to the axial component $E_Z$ of the $E_N$ field (see Fig. 11), a velocity component in the direction of the axis of the deflection cone may be superimposed on the electrons moving with a supposed constant velocity $v_o$ from the deflection plane to the observation plane. Electrons accelerated or decelerated in this way would cause no trouble if the only problem were to locate them properly with respect to their original phase angle. The only possible trouble would arise if one made a velocity analysis of a particular phase increment $\Delta\theta$ after the electrons are circularly spread and shot through a velocity analyzer, provided in the beam analyzer built in this laboratory.

In this case one would observe velocity spreads of electrons which originally had exactly the same velocity. To estimate this aberration due to the space charge action of the circularly deflected beam one has to set up the equation of motion for an edge electron moving in the direction of the axis of the cone.

Referring again to Fig. 11 one can immediately write down the field in the z direction:

$$E_z = E_N \sin \psi \tag{66}$$

With

$$E_N = 2\pi\rho b \tag{31}$$

$$b = r \cos \psi \tag{17}$$

$$\rho = \rho_o \frac{r_o^2}{r^2} \tag{23}$$

$$L = v_o t \tag{9a}$$

$$A = \frac{2\pi\rho_o e}{m_o v_o^2} \tag{43}$$

$$E_z = \frac{m_o}{e} \frac{d^2 z}{dt^2} \tag{67}$$

equation (66) becomes

$$\frac{d^2 z}{dL^2} = A \frac{r_o^2}{r} \sin \psi \cos \psi \tag{68}$$

The two variables occurring in the above equation, r and z, can be correlated with the aid of Fig. 14. From this figure one reads

$$\left.\begin{aligned} z_o &= r_o \tan \psi \\ z^* &= r \tan \psi \\ z^* &= z_o + z \end{aligned}\right\} \tag{69}$$

and thus

$$r = r_o + \frac{z}{\tan \psi} \tag{70}$$

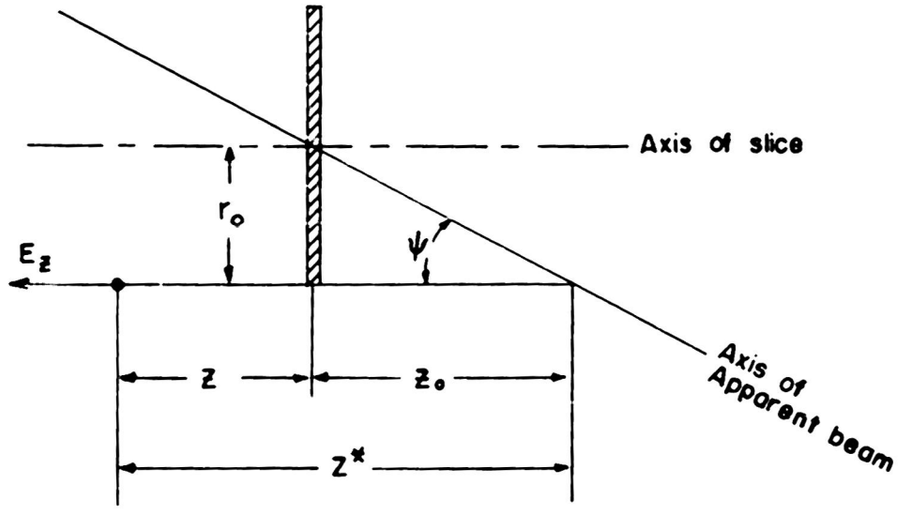


FIGURE 14

Replacing r in Eq. (68) by expression (70) one obtains

$$\frac{d^2z}{dL^2} = Ar_o^2 \frac{\tan\psi}{r_o \tan\psi + z} \sin\psi \cos\psi \tag{71}$$

Introducing the new variables

$$\begin{aligned} z/r_o &= \zeta \\ L/L_o &= \xi \end{aligned} \tag{72}$$

and using the expressions for sin ψ, cos ψ, and tan ψ as they were given in Eqs. (12) and (13)

$$\sin\psi = \frac{L/L_o}{\sqrt{1 + (L/L_o)^2}}$$

$$\cos\psi = \frac{1}{\sqrt{1 + (L/L_o)^2}} \tag{13}$$

$$\tan\psi = L/L_o \tag{12}$$

the differential equation (71) reduces to

$$\zeta'' = AL_o^2 \cdot \frac{1}{\zeta + \xi} \frac{\zeta}{1 + \xi^2} \tag{73}$$

Again this differential equation does not occur in literature and must be solved numerically or graphically. One can, however, find a reasonably good approximation by neglecting ζ with respect to ξ in the denominator of the first term in Eq. (73). Physically it means that the

displacement in the z direction will be very small in comparison with the distance from the deflection plane. Since this is actually the case, (73) reduces to

$$\zeta'' = AL_o^2 \frac{\xi}{1 + \xi^2} \tag{74}$$

and the first integral gives

$$\zeta' = AL_o^2 \ln\sqrt{1 + \xi^2} \tag{75}$$

Going back to the old variables z and L as defined in (72) and expressing $\zeta'$ in terms of the relative velocity spread,

$$\frac{\Delta v_z}{v_o} = \frac{1}{v_o} \frac{dz}{dt} = \frac{\Delta \beta_z}{\beta} \tag{76}$$

(75) becomes

$$\frac{\Delta \beta_z}{\beta} = AL_o r_o \ln \sqrt{1 + (L/L_o)^2} \tag{77}$$

The coefficient of the logarithm is a dimensionless product. It can be recognized as

$$\frac{2}{\pi} \Delta\theta_\infty \tan \alpha \qquad \text{(See Eq. (62)).}$$

Expressing $\Delta\theta_\infty$ conveniently according to Eq. (62) one obtains for the relative velocity modulation of the circularly deflected beam behind the deflection plane the expression

$$\frac{\Delta \beta_z}{\beta} = 1.88 \times 10^{-6} \frac{I_A}{\beta^2} \frac{\lambda}{r_o} \sin \alpha \ln \sqrt{1 + (L/L_o)^2} \tag{78}$$

Two features of this formula can easily be seen:

a) For zero deflection angle, $\alpha$, the velocity spread $\Delta\beta_z/\beta$ becomes zero, because sin $\alpha$ goes to zero. In other words, a straight undeflected cylindrical electron beam produces no velocity spread in the z direction.

b) The velocity spread increases slowly with increasing distance L from the deflection plane, viz. only with the logarithm of L.

Example

$I = 100$ mA
$r_o = 1$ mm
$\lambda = 10$ cm
$\alpha = 6°$
$L = 20\ L_o$
$\beta = 0.1$
$U_o = 2.5$ Kv

$$\frac{\Delta \beta_z}{\beta} = 5.6 \times 10^{-3}$$

Since

$$\frac{\Delta \beta_z}{\beta} = \frac{\Delta v_z}{v_o} = \frac{1}{2} \frac{\Delta U_z}{U_o}$$

in this example

$$\Delta U_z = 28 \text{ volts.}$$

# CHAPTER II

# CHROMATIC ABERRATIONS IN A DEFLECTING SYSTEM OF FINITE EXTENSION

## SYMBOLS

| | |
|---|---|
| $A, B$ | constants, defined by the geometry of a single pair of a Lecher system |
| $E_x, E_y$ | electric fields on the X and Y deflectors |
| $L$ | distance deflector-screen |
| $P$ | electric power fed into the deflector |
| $R$ | radius of the circle of the circularly deflected beam |
| $U_o$ | beam voltage |
| $U_*$ | zero radial displacement voltage |
| $a, b$ | major and minor axes of an ellipse |
| $\varepsilon$ | eccentricity of an ellipse |
| $a, b$ | axial displacement and radius of a single pair of a Lecher system |
| $s_I$ | aperture of a Lecher system |
| $s_{II}$ | spacing of two Lecher systems |
| $x, y$ | coordinates of an electron hitting the observation plane |
| $\xi, \eta$ | coordinates at 45° angles with x, y |
| $\varphi_1$ | transit angle of an electron traveling between two Lecher Systems |
| $\varphi_{1o}$ | transit angle of an electron traveling with the velocity of the beam voltage between the Lecher systems |
| $\Delta\theta$ | an angular displacement |
| $\varphi$ | phase of the oscillating X-deflector |
| $\varphi_1$ | a tunable phase |
| $\delta$ | an unadjustable phase angle |
| $\alpha$ | deflection angle between the undeflected and deflected beam |
| $\gamma$ | the apparent deflection in a plane perpendicular to the undeflected beam |

# 1. INTRODUCTION

To distinguish aberrations which could stem from different causes, the assumption of an idealized infinitesimally thin "deflection plane" was made in the preceding chapter. This is, of course, not true. Every realizable deflection system must have a finite extension to allow the deflecting forces a finite time to accelerate the particle in the direction of the force. In the particular case of the "phase writer system" of the beam analyzer, the extension of the system is given by the distance of the two pairs of the Lecher wires which provide deflections in two rectangular coordinates. The effect of this extension on electrons with different velocities (polychromatic electron beam) has been briefly touched upon in Progress Report 13 of this contract. In the following pages a more detailed account of this type of aberrations will be given.

## 2. RADIAL DISPLACEMENT

The principle of the deflecting mechanism consists of two pairs of shorted Lecher wires, placed perpendicular to each other and excited in such a manner that the maxima of the standing waves on both wire pairs fall on the cross point of the pairs. The electron beam is shot through the little square-shaped window which is formed by the edges of the wires. (See Fig. 1.) If the two wire pairs are sufficiently far

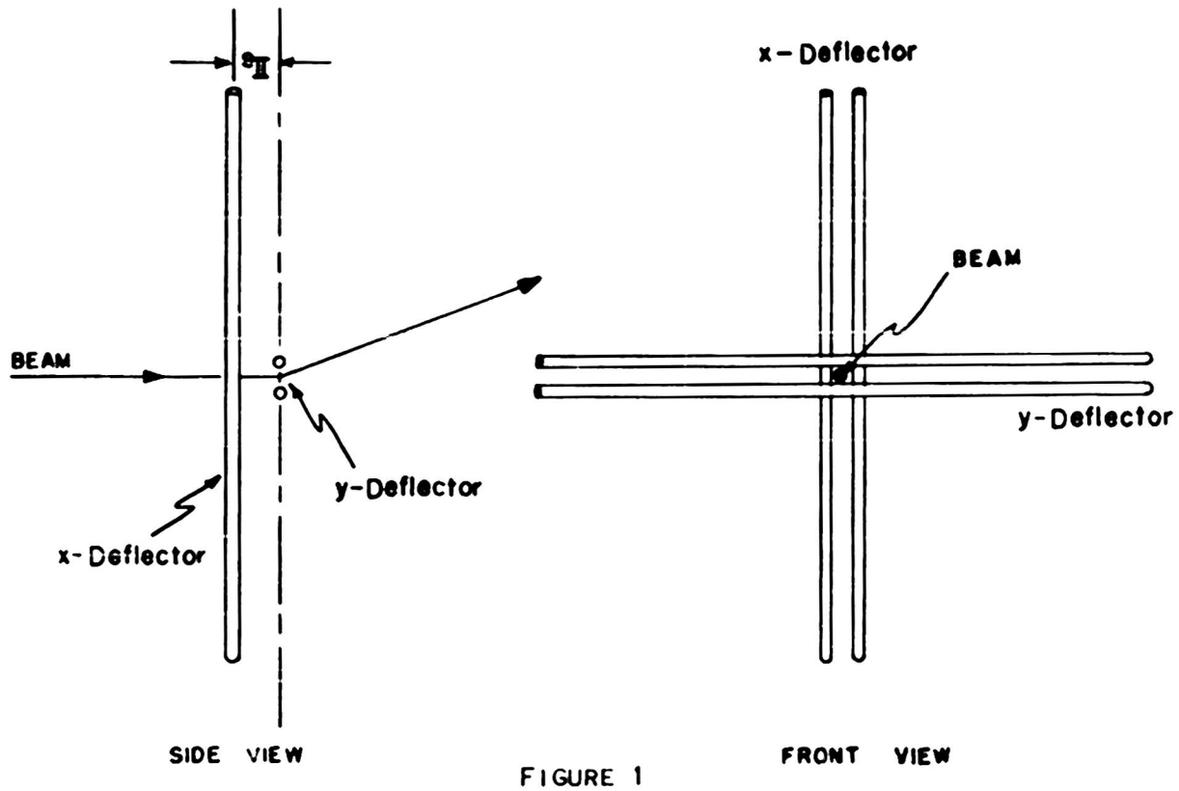


FIGURE 1

apart (about twice the spacing of the two wires in either pair), then it is possible to excite each part independent of the other. Using the first deflecting system as deflector in the x direction and as a reference plane for the phase at any point along the beam axis, the field at the cross point will follow the expression

$$E_x = E_{xo} \cos \varphi \qquad (1)$$

The field for the Y deflector may be expressed by

$$E_y = E_{yo} \sin (\varphi - \varphi_1) \qquad (2)$$

where $\varphi_1$ is an adjustable phase difference between the X and Y deflector.

Now consider an electron passing through the X deflector. As was shown in Progress Report No. 12, it will be deflected at an angle, the tangent of which is proportional to the instantaneous field on the wire. Thus an electron passing the X deflector at a phase angle $\varphi$ will hit the observation plane at a point with the coordinate

$$x = R \cos \varphi. \qquad (3)$$

The same electron has to pass the Y deflector, but will do so a little later. Let the phase difference of the arrival of the electron at the X deflector and Y deflector be

$$\phi_1 = \omega t_1 = 2\pi \frac{s_{II}}{\lambda} \frac{c}{v} \tag{4}$$

where

$s_{II}$ is the spacing of the two wire pairs

c is the velocity of light

v is the velocity of the electron,

and let the magnitude of the oscillating fields and the two pairs be exactly the same--a condition easily realizable in any particular system

$$E_{xo} = E_{yo} \tag{5}$$

Then the deflection in the y direction will follow the equation

$$y = R \sin (\varphi - \varphi_1 + \phi_1) \tag{6}$$

Since $\varphi_1$ is an adjustable phase difference, $\varphi_1$ can be adjusted such that

$$\varphi_1 = \phi_1 \tag{7}$$

and a uniform electron beam will display itself on the observation screen as a perfect circle following the equation

$$\begin{aligned} x &= R \cos \varphi \\ y &= R \sin \varphi \end{aligned} \tag{8}$$

Assume now that the electron beam would not be a monochromatic one, i e. a beam consisting of electrons having one and only one velocity, viz. $v_o$, but would consist of electrons having velocities v spread over a range between $v_o + \Delta v$ and $v_o - \Delta v$ For those electrons the phase difference of arrival at the X and Y deflector would be

$$\phi_1 = 2\pi \frac{s_{II}}{\lambda} \frac{c}{v_o \pm \Delta v} \tag{9}$$

Assuming $\Delta v << v_o$ and expanding the denominator one obtains

$$\phi_1 = 2\pi \frac{s_{II}}{\lambda} \frac{c}{v_o} \left(1 \mp \frac{\Delta v}{v_o}\right) \tag{10}$$

and using (4)

$$\phi_1 = \phi_{1o} \mp \phi_{1o} \frac{\Delta v}{v_o}, \tag{10a}$$

where

$$\phi_{1o} = 2\pi \frac{s_{II}}{\lambda} \frac{c}{v_o} . \tag{11}$$

Inserting the phase difference $\phi_1$ into Eq. (6) for the y deflection, the y coordinate becomes

$$y = R \sin (\varphi - \varphi_1 + \varphi_{10} \mp \varphi_{10} \frac{\Delta v}{v_o}). \tag{12}$$

Although it is possible to compensate $\phi_{10}$, by adjusting $\varphi_1$ so that

$$\varphi_1 - \phi_{10} = 0,$$

it is impossible to compensate for the phase spread $\phi_{\theta_1} \frac{\Delta v}{v_o}$, because any $\Delta v$ can occur at any instant $\varphi$. Adjusting for $\phi_{10}$, Eq. (12) becomes

$$y = R \sin (\varphi \mp \phi_{10} \frac{\Delta v}{v_o}) \tag{13}$$

with the unadjustable phase

$$\delta = \mp \phi_{10} \frac{\Delta v}{v_o} \tag{14}$$

The existence of such an unadjustable phase angle $\delta$ is due to two causes:

a) the polychromacy of the beam; for, if the beam were monochromatic, $\Delta v = 0$, then $\delta$ would vanish.

b) the finiteness of the spacing of the two wire pairs, for, if $s_{II}$ were zero, $\phi_{10}$ would be zero (see Eq. (4)), then $\delta$ would vanish.

Therefore the existence of $\delta$ is due to a chromatic beam deflected by a deflecting system of a finite extension. The effect of the existence of $\delta$ can be seen immediately.

Consider again an electron passing the X deflector at a phase angle $\varphi$ and having a velocity $v_o - \Delta v$. It will be projected at a point P on the screen (see Fig. 2) with the coordinates

$$x = R \cos \varphi \tag{15}$$

$$y = R \sin (\varphi + \delta) \tag{16}$$

Electrons arriving at any phase $\varphi$ at the X deflector will define the set of all points given in Eq. (15) (16) with $\varphi$ as the parameter.

It can easily be shown that these points define an ellipse, the axes of which make a 45° angle with the coordinates xy. The major axis, the minor axis, and the eccentricity are defined by the following relations

$$a = R \sqrt{1 + \sin \delta} \tag{17}$$

$$b = R \sqrt{1 - \sin \delta} \tag{18}$$

$$\varepsilon = R \sqrt{2 \sin \delta} \tag{19}$$

See Fig. 3 and Appendix A.

For evaluating Eqs. (17) and (18) most conveniently, a nomograph is included (Fig. 4), which makes it possible to determine a and b if $\Delta v/v_o$ and $\phi_o$ are given, or, if a and b are measured from a particular

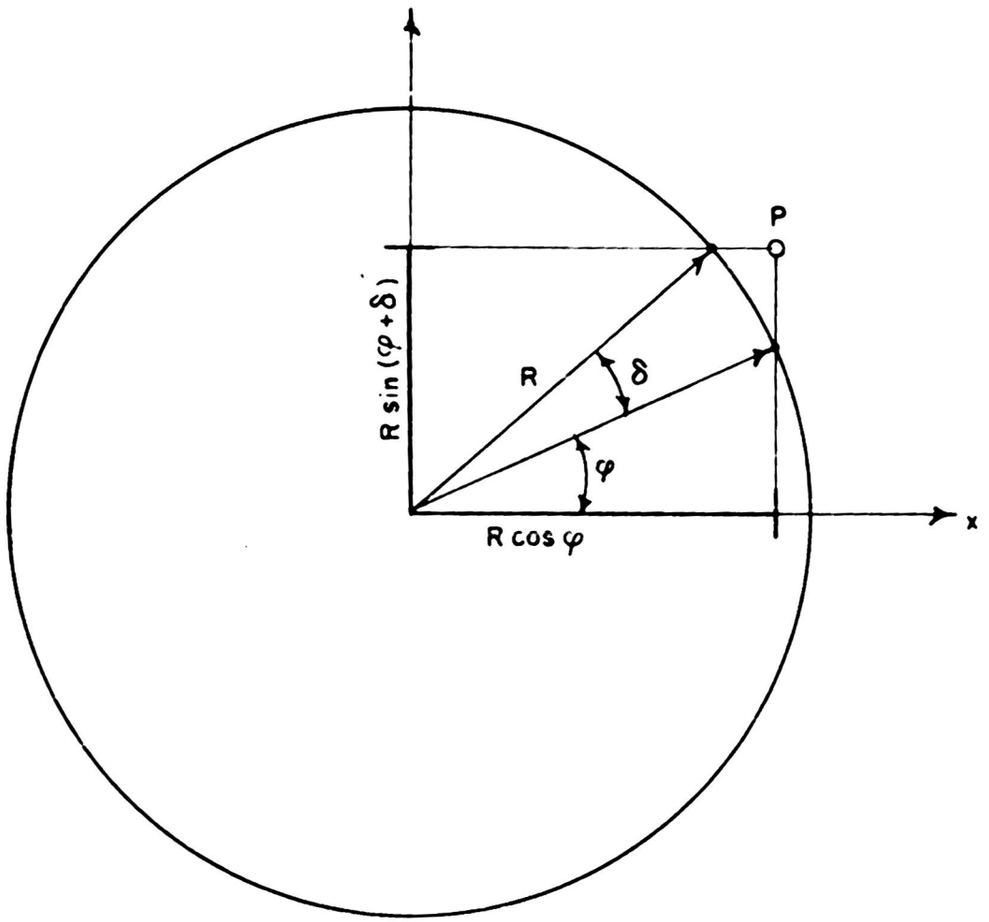


FIGURE 2

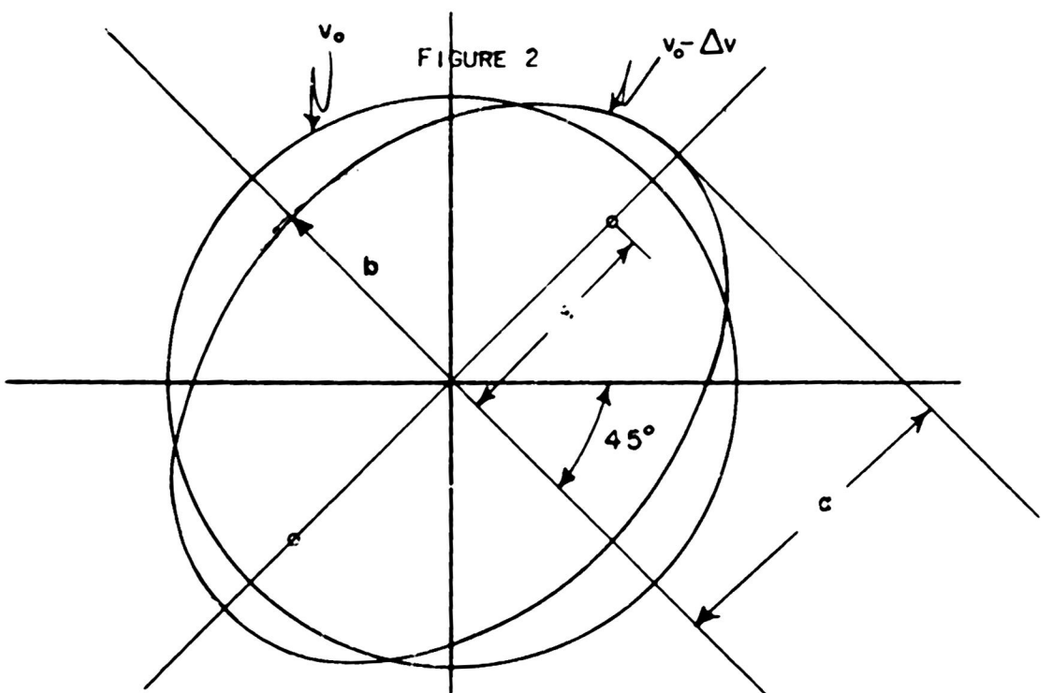


FIGURE 3 THE LOCUS OF ALL POINTS DEFINED BY ARRIVING ELECTRONS HAVING A VELOCITY $v = v_o - \Delta v$

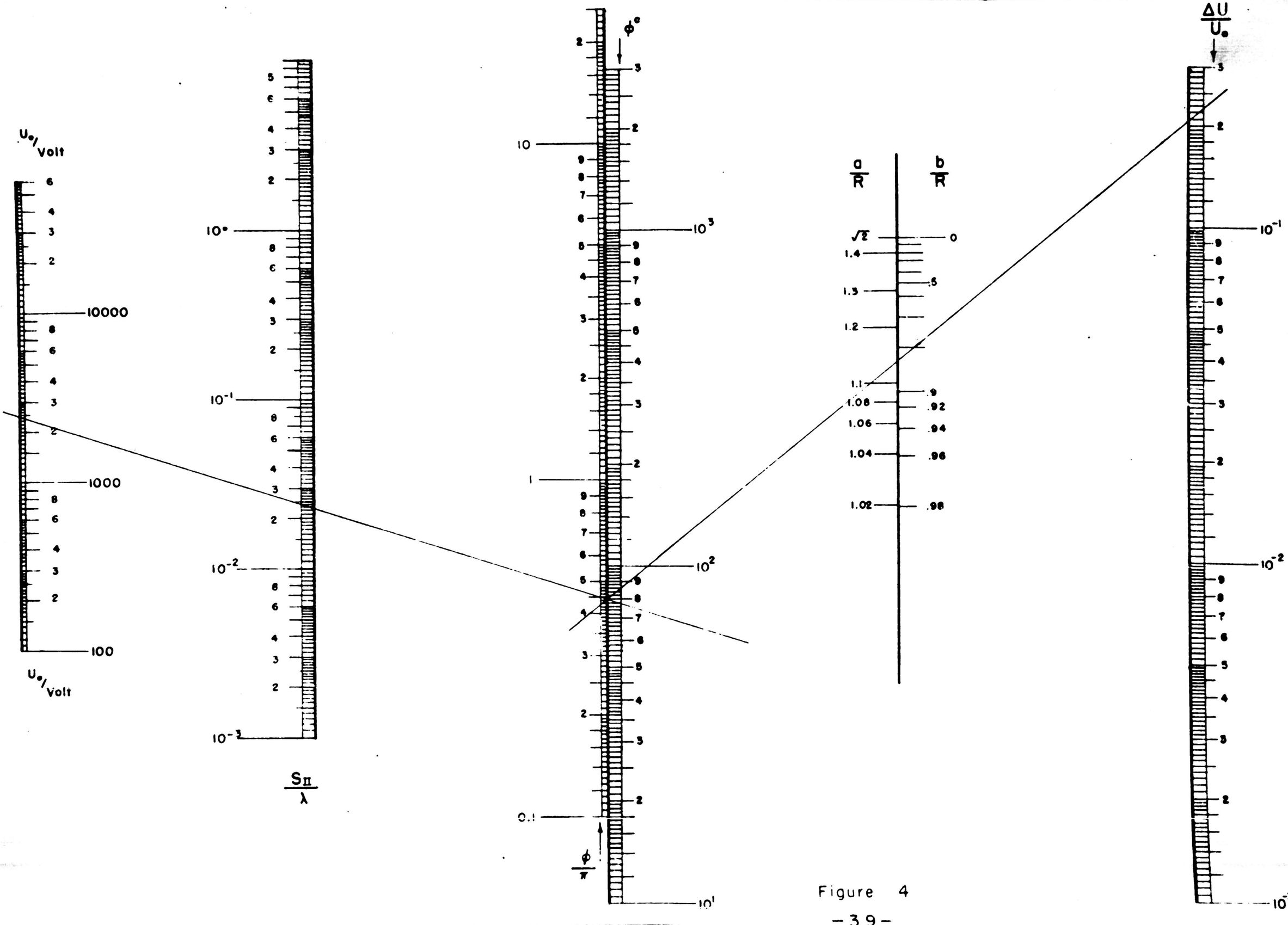
$U_e$/Volt
10000
1000
100
$U_e$/Volt
$10^0$
$10^{-1}$
$10^{-2}$
$10^{-3}$
$\frac{S_{II}}{\lambda}$
10
$10^3$
1
$10^2$
0.1
$10^1$
$\frac{\phi}{\pi}$
$\phi^o$
$\frac{a}{R}$
$\frac{b}{R}$
$\sqrt{2}$
0
1.4
.5
1.3
1.2
1.1
.9
1.08
.92
1.06
.94
1.04
.96
1.02
.98
$\frac{\Delta U}{U_e}$
$10^{-1}$
$10^{-2}$
$10^{-3}$

Figure 4

experiment, to determine the velocity spread $\Delta v/v_o$. To have $\phi_o$ easily available, this nomograph also makes it possible to determine $\phi_o$ immediately, if $v_o$ and the geometry of the system, viz. $s_{II}/\lambda$ are given.

For electrons having a velocity $v_o + \Delta v$ ("fast case"), the locus of all points of their arrival will be an ellipse perpendicular to the former one, but with precisely the same a and b as in the "slow case" ($v = v_o - \Delta v$).

An electron beam with electrons spread over the range $v = v_o \pm \Delta v$ will thus project itself on the screen on an area which is limited by the two crossed ellipses and the fundamental circle as indicated in Fig. 5. This picture shows that even for an ideally focused electron

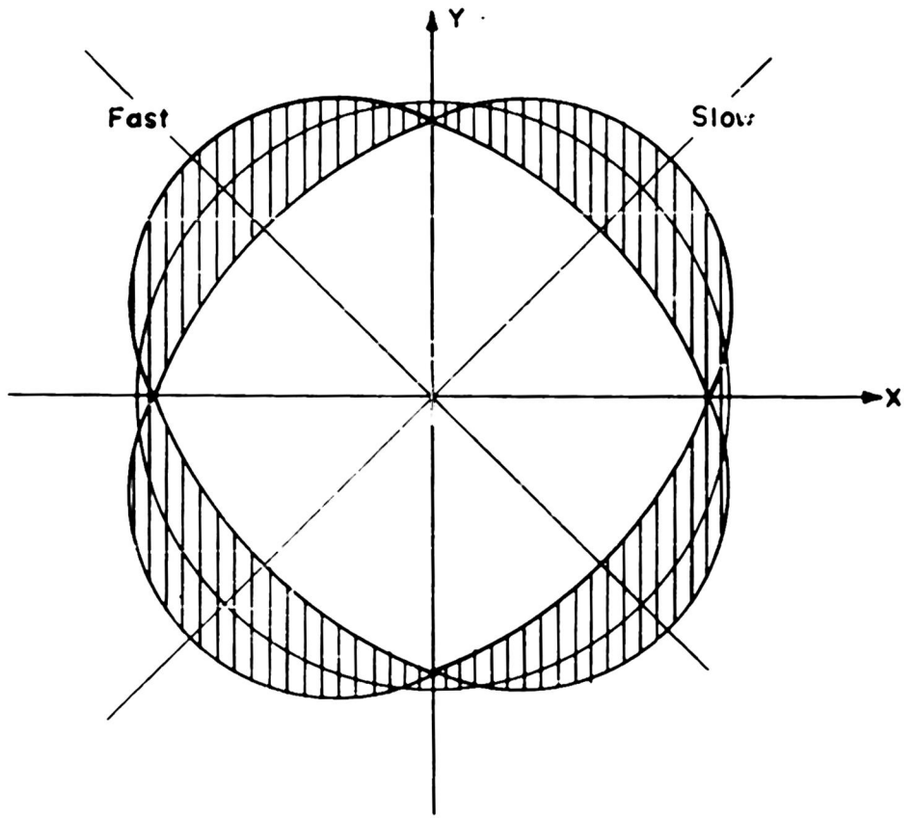


FIGURE 5

beam the observed beam width can be quite large. The maximum apparent beam width on the screen occurs along a line making a 45° angle with the x and y axes. Its width can be used to approximately determine an inherent velocity spread. Since the maximum apparent beam diameter, $d^{II}_{app}$, is the difference of the major and the minor axes of the fast and

the slow ellipse, from Eqs. (17) and (18) an expression in terms of the velocity spread can easily be established. Defining

$$d^{II}_{app} = a - b \tag{20}$$

and inserting from (17) and (18) the expressions for a and b, after simple trigonometric transformations one obtains for the apparent beam diameter

$$d^{II}_{app} = 2R \sin \frac{\delta}{2} \tag{21}$$

Since $d^{II}_{app}$ and R are directly measurable, $\delta$ can be found from Eq. (21). With

$$\delta = \phi_{1o} \frac{\Delta v}{v_o} \tag{14}$$

and

$$v = kU^{1/2}$$

$$dv = \tfrac{1}{2} kU^{1/2} dU$$

$$\frac{\Delta v}{v_o} = \frac{1}{2} \frac{\Delta U}{U_o} \tag{22}$$

the velocity spread expressed in electron volts becomes

$$\frac{\Delta U}{U_o} = \frac{4}{\phi_{1o}} \text{ arc sin } \frac{d^{II}_{app}}{2R} \tag{23}$$

In the preceding pages there was, of course, no suggestion to use this method of measuring the beam width to determine accurately the velocity spread in an electron beam. The sole purpose of this consideration was to give this phenomenon, which eventually could occur, a proper interpretation, and also to give the experimenter a hint to estimate an existent velocity spread in the beam. Means of accurately determining the velocity spectrum of an electron beam have to follow entirely different lines. (See Progress Report No. XIX-14.)

This section, dealing with chromatic aberrations of an electron beam deflected by a system of finite extension, would not be complete if the influence of the finiteness of a single wire pair, say the X deflector alone, were not studied. In fact, the deflection sensitivity of a single pair of wires shows a dependency of the velocity of the injected electrons. In Progress Report No. XIX-12 this influence was reported and studied. If one calls

$\alpha$ the deflection angle of the injected beam

P the power delivered to the wires

then the sensitivity of a single pair of wires follows a formula of the form

$$\tan \alpha = \sqrt{P} \frac{A}{U} e^{-B/\sqrt{U}} \tag{24}$$

where U is the velocity of the injected electrons expressed in electron volts and A and B are quantities defined by the geometry of the wires.

$$A = \frac{2\ 07\ \frac{\lambda}{a}}{\sqrt{1 + 4.75 \times 10^{-7}\ \frac{\lambda}{b}\sqrt{\frac{\lambda^3}{a^2 - b^2}}}} \tag{25}$$

$$B = \frac{\pi}{2}\ 10^3\ \frac{s_I}{\lambda}\sqrt{1 + 4\ \frac{b}{s_I}} \tag{26}$$

The symbols a, b, and D, used in Eqs (25) (26) are explained in Fig 6

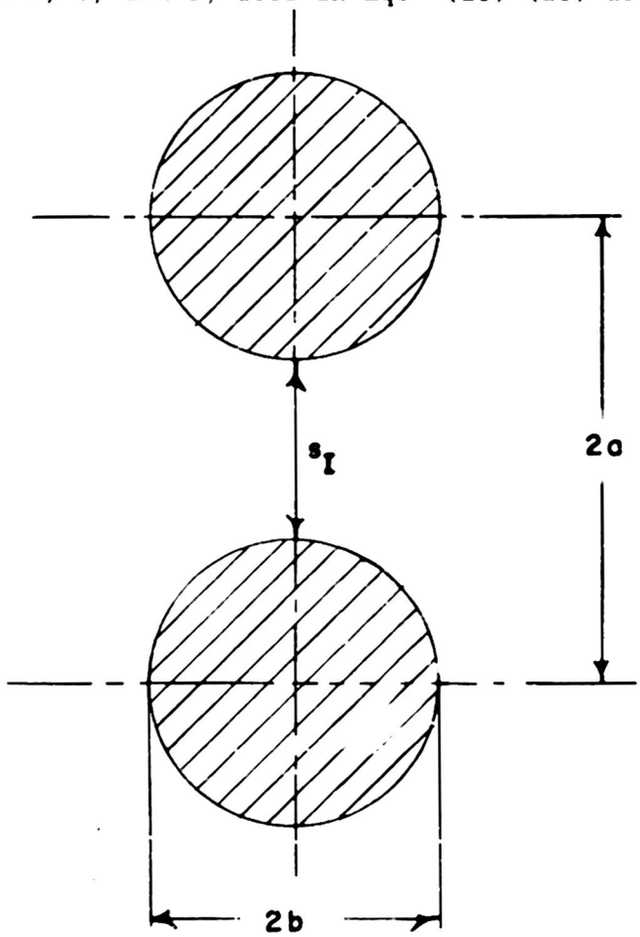


FIGURE 6

Equation (24) is plotted in Fig 7 for a particular system which was built and experimentally checked in this laboratory

Since tan $\alpha$ = R/L, (see Fig 3, of the preceding chapter) and during a particular experiment the power, P, delivered to the system and its geometrical dimensions are kept constant, Eq (24) can be trans-

formed into a statement about the relation of the radius R of the circularly deflected beam on the screen and the velocity of the electrons at the deflection system

$$R = \frac{K}{U} e^{-B/\sqrt{U}} \tag{27}$$

where $K = AL\sqrt{P}$ is a constant

Differentiating R with respect to U gives the variation of the deflection radius with respect to a velocity change

$$\frac{dR}{dU} = -\frac{K}{U^2} e^{-B/\sqrt{U}} + \frac{K}{U} e^{-B/\sqrt{U}} \left( \frac{B}{2U^{3/2}} \right) \tag{28}$$

Using Eq (27) again one obtains the relative radial displacement

$$\frac{\Delta R}{R} = \frac{\Delta U}{U_o} \left( \frac{B}{2\sqrt{U_o}} - 1 \right) \tag{29}$$

For a particular voltage $U_*$ the radial displacement vanishes if

$$\frac{B}{2\sqrt{U_*}} = 1 \tag{30}$$

This defines $B^2$ in terms of a voltage and (29) becomes

$$\frac{\Delta R}{R} = \frac{\Delta U}{U_o} \left( \sqrt{\frac{U_*}{U_o}} - 1 \right) \tag{31}$$

$U_*$ is directly connected with Eq (26) through Eq (30) and thus is predetermined by the designer Reasonable values of $U_*$ turn out to be in the neighborhood of about 500 volts (see Fig 7) Since electron beams are usually operated at somewhat higher voltages one will find oneself on the right hand side of the curve, where increasing velocities decrease the sensitivity of the system But even at about 3000 volts, the loss in sensitivity is not too strong and can still easily be compensated by an increase of the power P fed into the system

Let us consider again a velocity spread of $\pm\Delta v$ In a similar manner as before an apparent beam diameter $d^I_{app}$ can be defined due to a change in the deflection sensitivity of the system This beam width would occur even for an ideally focused beam Assuming one operates with velocities above the zero displacement voltage $U_*$ and defining

$$d^I_{app} = 2\Delta R \tag{32}$$

one obtains with (31)

$$d^I_{app} = R \frac{\Delta U}{U_o} \left( 1 - \sqrt{\frac{U_*}{U_o}} \right) \tag{33}$$

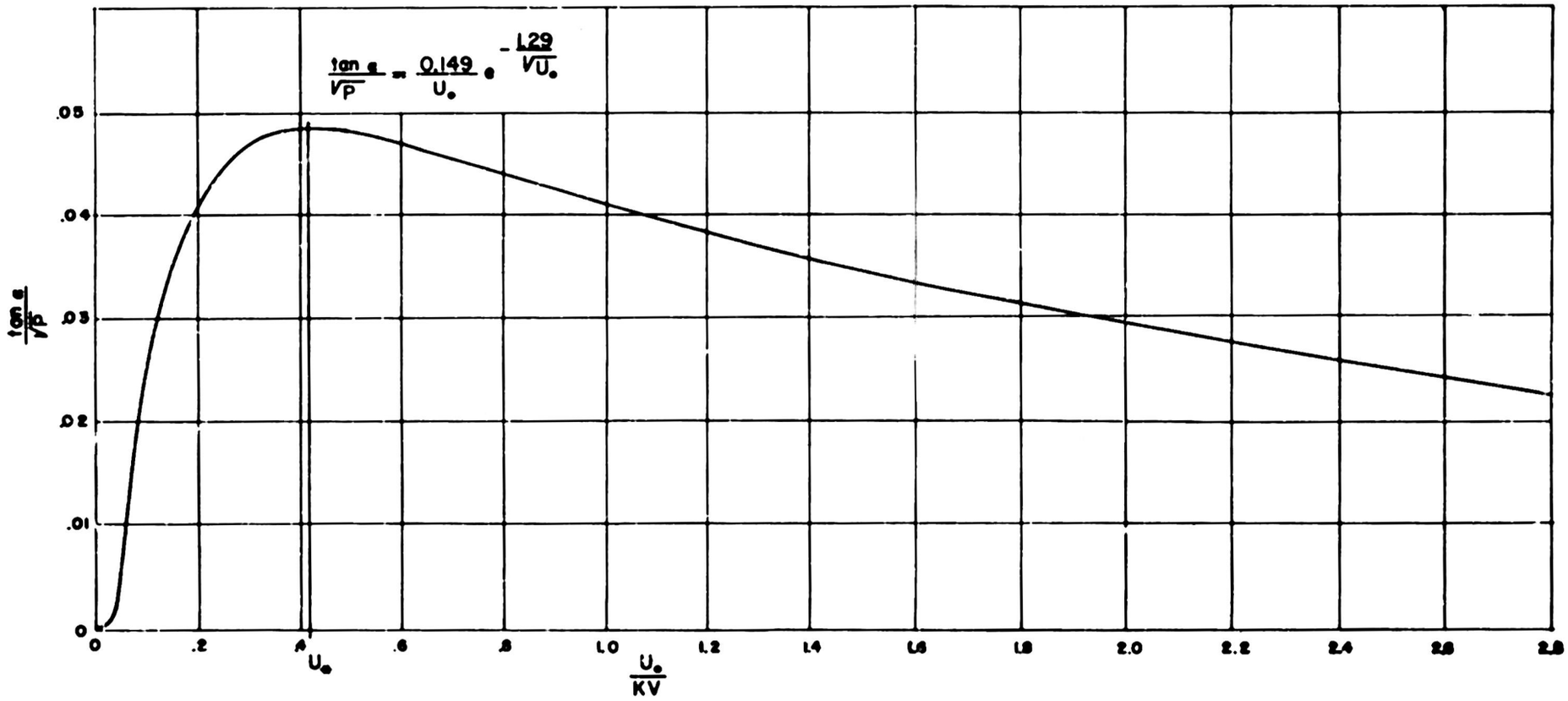


Graph of Deflection Vs. Beam Voltage
for the Deflection System of the Phase Writer

Figure 7

This equation describes an apparent beam spread due to a finite extension of a single deflector, and is exactly the equivalent of Eq (21), which predicted a beam spread for a system consisting of two such deflectors with finite spacing.

It may be interesting to compare their influence on the apparent beam diameter. Allowing the approximation

$$\sin z \sim z$$

for small z, Eq (21) becomes

$$d^{II}_{app} = R\phi_{01} \frac{\Delta U}{2U_o} \tag{34}$$

Defining a quantity

$$\kappa = \frac{\text{diameter for double system}}{\text{diameter for single pair}} = \frac{d^{II}_{app}}{d^{I}_{app}} \tag{35}$$

and using Eqs (33) and (34) one gets

$$\kappa = \frac{\phi_{10}}{2(1 - \sqrt{U_*/U_o})} \tag{36}$$

To arrive at a more convenient form for $\kappa$, Eq (11) for $\phi_{10}$ and Eq (30) in combination with (26) for $U_*$ may be used $\kappa$ finally becomes

$$\kappa = \frac{2s_{II}}{s_I} \cdot \frac{1}{\sqrt{1 + 4\frac{b}{s_I}}} \cdot \frac{1}{\sqrt{U_o/U_*} - 1} \tag{37}$$

This equation contains only geometrical quantities and the applied beam voltage in units of the zero displacement voltage $U_*$

For a practical system, e g ,

$s_I = 1.5$ mm $\qquad U_o = 1000$ V

$s_{II} = 5.0$ mm $\qquad U_* = 500$ V

$b = 1.0$ mm

one obtains

$$\kappa = 3.5$$

This indicates that the apparent beam spread due to the spacing of the two deflectors is 3.5 times greater than a beam spread due to the change in sensitivity of a single deflector, independent of the velocity spread $\Delta U$

For experimental confirmation of the described phenomena see Appendix B

## 3. ANGULAR DISPLACEMENT

In the preceding section it was shown that due to a finite distance between the X and Y deflectors an electron $\Delta v$ faster or slower than the average electron in a beam will impinge on the screen, not on a circle drawn by the average electron, but will be somewhat displaced. Having already computed the radial displacement of such electrons, in this paragraph the angular displacement may be considered. By angular displacement one has to understand again the phenomenon that an electron belonging to a particular phase increment, say $\varphi$, will show up on the screen in a phase increment, $\varphi + \Delta\varphi$, different from the one to which it belonged when it entered the deflection system. The quantity $\Delta\theta$ will be computed here.

As it was already pointed out a velocity spread of $\pm\Delta v$ will produce two ellipses on the screen with the equations

$$x = R \sin \varphi \tag{15}$$

$$y = R \sin (\varphi + \delta) \tag{16}$$

where $\delta$ is defined as

$$\delta = \mp \phi_{10} \frac{\Delta v}{v_o} \tag{14}$$

The sign of $\delta$ determines the position of the ellipse.

With the aid of Fig. 8 the significance of the angular displacement in this context can easily be observed. Instead of being projected on

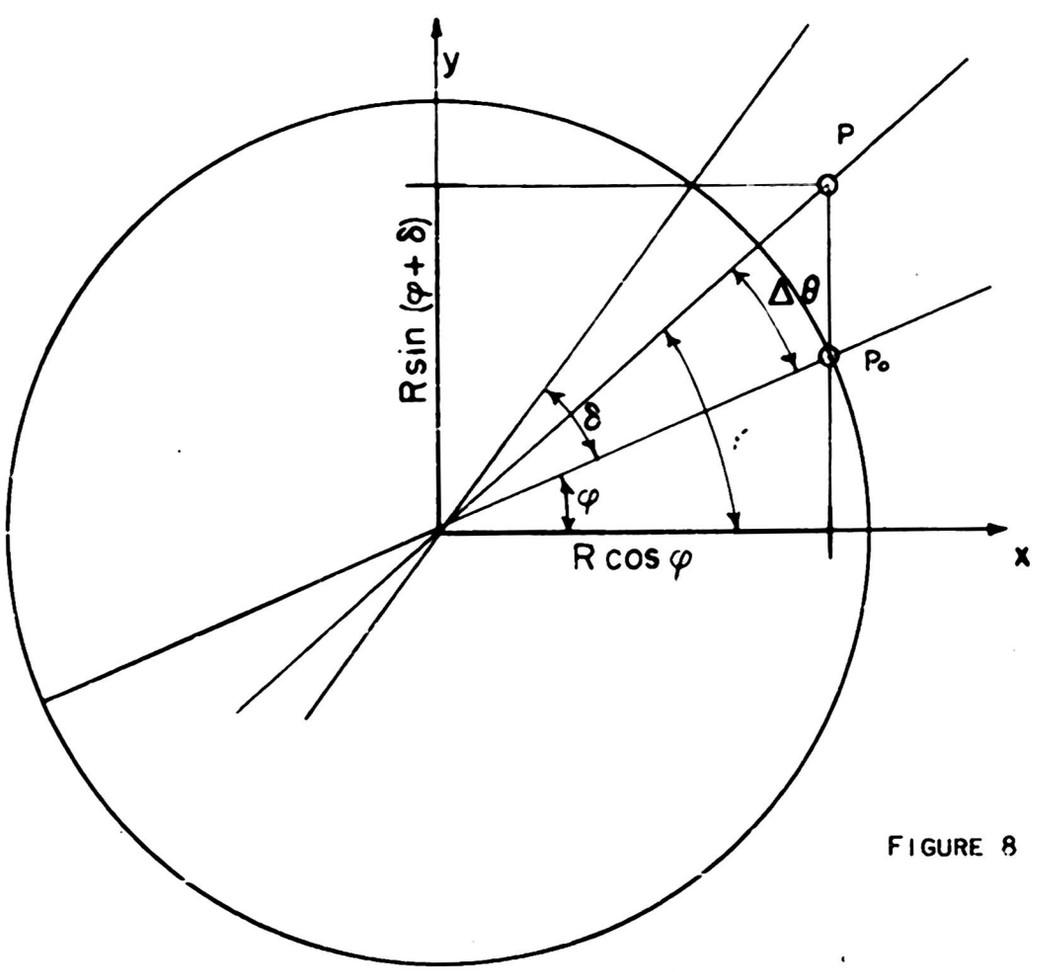


FIGURE 8

point $P_o$, if the unadjustable phase angle $\delta$ is not zero, the electron arrives at point P, causing an angular displacement $\Delta\theta$.

With Fig. 8 the following two relations can be derived:

$$\tan \gamma = y/x \tag{38}$$

$$\Delta\theta = \gamma - \varphi \tag{39}$$

Inserting for x and y the expressions (15) and (16), eliminating $\gamma$ with (39) and solving for $\Delta\theta$, one obtains after simple trigonometric transformations

$$\tan \Delta\theta = \frac{\sin \delta - \tan \varphi(1 - \cos \delta)}{1 + \tan^2 \varphi \cos \delta + \tan \varphi \sin \delta} \tag{40}$$

The above equation is already the answer to the question of the angular displacement. It shows the dependency of $\Delta\theta$ on the original phase angle and the unadjustable phase $\delta$.

It is interesting to note that $\tan \Delta\theta$, and thus $\Delta\theta$, can vanish. This is the case if

a) the denominator goes to infinity

b) the numerator goes to zero

The first condition is fulfilled if

$$\tan \varphi = \infty$$

or

$$\varphi = \pm \frac{\pi}{2} . \tag{41}$$

In other words, no angular displacement occurs at the y axis. The second condition is fulfilled if

$$\sin \delta = \tan \varphi \, (1 - \cos \delta) \tag{42}$$

Solving for $\tan \varphi$, one obtains after using the trigonometric relations for half angles

$$\tan \varphi = \tan \left( \frac{\pi}{2} - \frac{\delta}{2} \right) \tag{43}$$

$$\varphi = \tfrac{1}{2} (\pi - \delta). \tag{44}$$

The following graph (Fig. 9) and the sketch (Fig 10) show the angles along the circle where no angular displacement occurs.

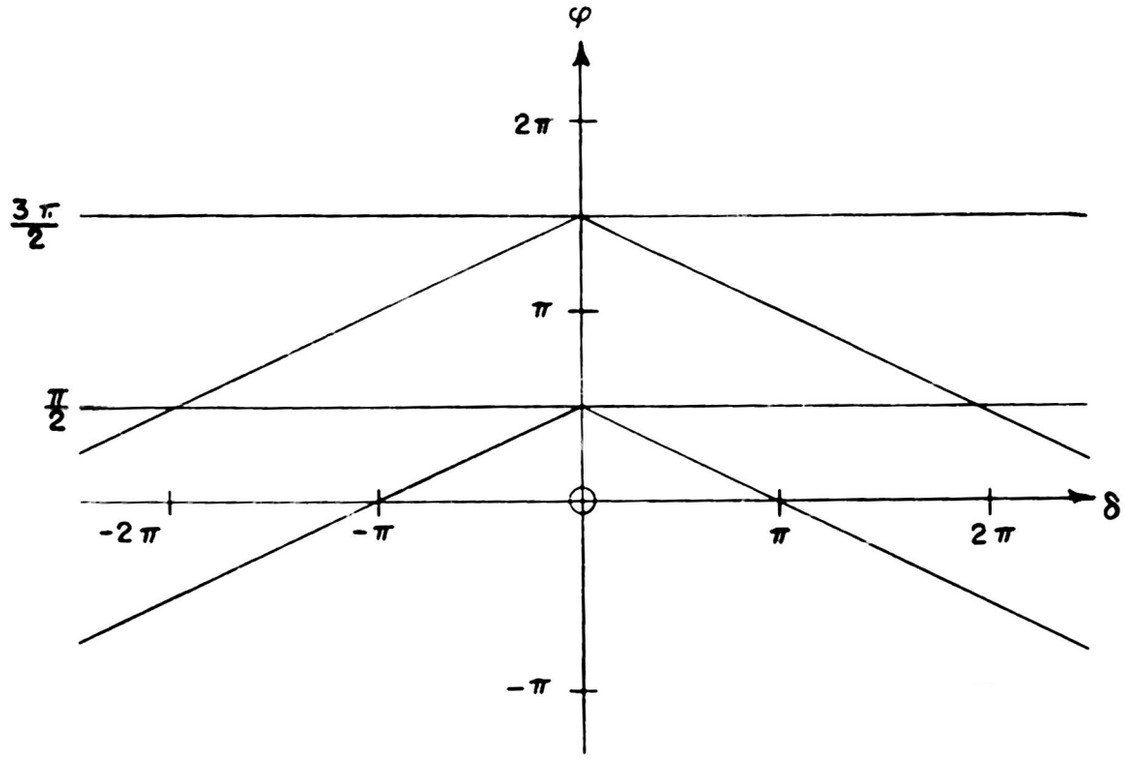


FIGURE 9

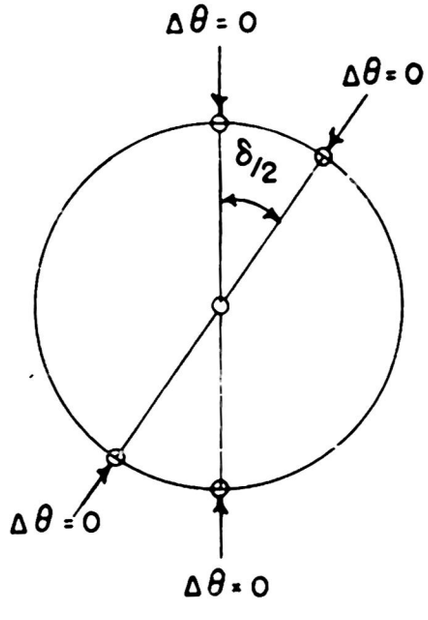


FIGURE 10

## APPENDIX A

Eliminate $\varphi$ from the equations

$$x = R \cos \varphi \tag{15}$$

$$y = R \sin (\varphi + \delta) \tag{16}$$

With

$$\sin(\varphi + \delta) = \sin \varphi \cos \delta + \cos \varphi \sin \delta$$

and

$$\cos^2 \varphi = (x/R)^2$$

$$\sin^2 \varphi = 1 - (x/R)^2$$

one obtains

$$y^2 - 2xy \sin \delta + x^2 = R^2 \cos^2 \alpha \tag{A1}$$

Introducing a new coordinate system $\xi$, $\eta$, which makes an angle $\gamma$ with the xy system, the following transformation can be established: (see Fig. A1)

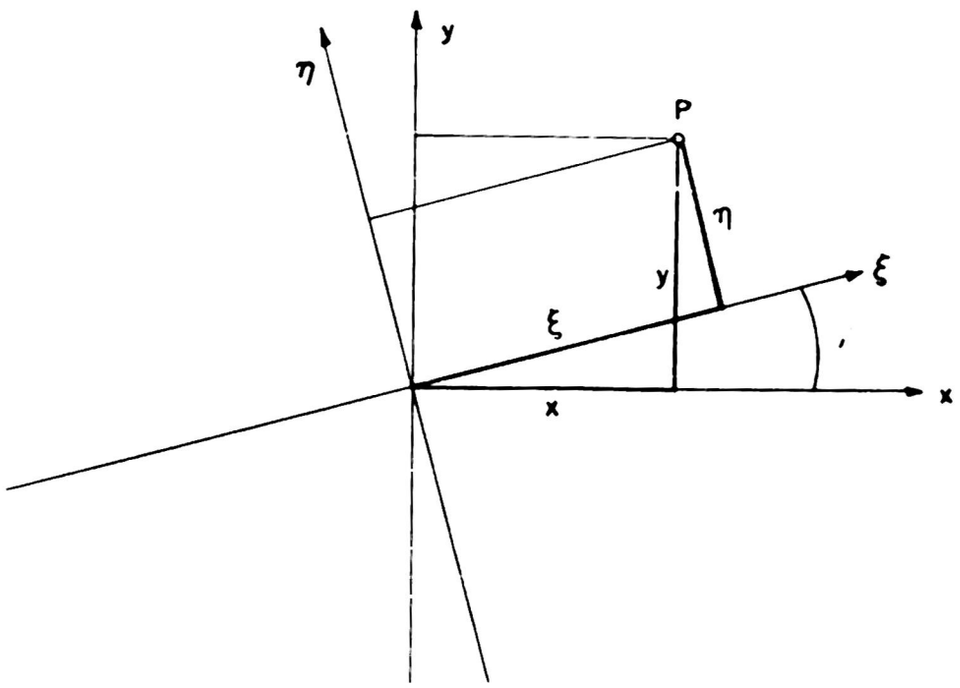


FIGURE A1

$$x = \xi \cos \gamma - \eta \sin \gamma \tag{A2}$$

$$y = \eta \cos \gamma + \xi \sin \gamma$$

For $\gamma = 45°$, (A2) becomes

$$\sqrt{2}\, x = \xi - \eta$$

$$\sqrt{2}\, y = \xi + \eta \tag{A3}$$

Adding and subtracting gives

$$\xi = \frac{1}{\sqrt{2}} (x + y)$$

$$\eta = \frac{1}{\sqrt{2}} (y - x) \qquad \text{(A4)}$$

Defining in the new coordinates $\xi, \eta$ an ellipse:

$$\left(\frac{\xi}{a}\right)^2 + \left(\frac{\eta}{b}\right)^2 = 1, \qquad \text{(A5)}$$

and expressing $\xi$, $\eta$ in the old coordinates by using transformation (A4) one obtains

$$x^2 - 2\,\frac{a^2 - b^2}{a^2 + b^2}\,xy + y^2 = \frac{2a^2 b^2}{a^2 + b^2} \qquad \text{(A6)}$$

Comparison with (A1) gives

$$\sin\delta = \frac{a^2 - b^2}{a^2 + b^2} \qquad \text{(A7)}$$

$$R^2 \cos^2\delta = \frac{2a^2 b^2}{a^2 + b^2} \qquad \text{(A8)}$$

With

$\cos^2\delta = 1 - \sin^2\delta$ one obtains

$$\cos\delta = \frac{2ab}{a^2 + b^2} \qquad \text{(A9)}$$

thus

$$R = \sqrt{\frac{a^2 + b^2}{2}} \qquad \text{(A10)}$$

Solving for a and b, one gets immediately

$$a = R\sqrt{1 + \sin\delta} \qquad (17)$$

$$b = R\sqrt{1 - \sin\delta} \qquad (18)$$

quod erat demonstrandum.

With $\varepsilon^2 = a^2 - b^2$, the eccentricity is found to be

$$\varepsilon = R\sqrt{2\sin\delta} \qquad (19)$$

## APPENDIX B

In Section 2, "Radial Displacement", two different causes for the radial spread of a polychromatic beam were mentioned and treated separately, namely, displacements due to the finiteness of a single deflector system, and displacements due to a finite spacing of the two deflectors. In actual operation, however, both effects will act simultaneously on the beam and will be superposed.

With the preceding discussion in mind it is not too difficult to anticipate what will happen. Suppose the system is set for a perfect circular display of electrons having a velocity $U_o$. All electrons having a somewhat higher velocity, say $U_o + \Delta U$, will flip into their ellipse, denoted as the "fast case", but will at the same time suffer a decreased deflection due to the decreased sensitivity of the single system for higher velocities. Since the ellipse for the "slow case" is perpendicular to the "fast case", electrons with a smaller velocity, say $U_o - \Delta U$, will display themselves along an ellipse with increased sensitivity for slow electrons. The reference circle for both cases is directly predictable with Eq. (24) and thus the combined effects can be visualized easily, as is done in Fig. B1. Three monochromatic electron beams are displayed, with velocities $U_o$, $U_o + \Delta U$, and $U_o - \Delta U$. The system is adjusted to a circle for electrons with the velocity $U_o$. The increase and decrease of the single system sensitivity is taken into account by drawing the ellipses into the two reference squares $U_o + \Delta U$ and $U_o - \Delta U$.

To compare this theoretical picture with an actual display on the screen of the analyzer, three successive exposures of a monochromatic electron beam having the velocity of 2000 volts, 2000 + 200 volts, and 2000 - 300 volts were made on the same negative. The system was adjusted to a circle at $U_o$ = 2000 volts. The result is given in Fig. B2 and shows a good correspondence with the theory.

In Fig. B3 a polychromatic beam is shown having electrons with all velocities from 2000 - 400 volts up to 2000 + 400 volts. The circular adjustment was again made at 2000 volts. This picture drastically shows the effect of a velocity modulation on the "apparent beamwidth".

Figures B4 and B5 are again superpositions of four monochromatic beams, where the former shows the effect of increasing the beam velocity until the phase angle $\Phi_1$ between the two deflector systems decreases precisely $\pi/2$ to degenerate the ellipses into a straight line. The latter shows very markedly the effect of the increase of sensitivity by decreasing the velocity. Here too, the velocity was changed until the phase angle between the two deflectors was increased to the amount $\Phi_{o1} + \pi/2$.

In all photographs the frequency applied was 3000 M cycles/sec.

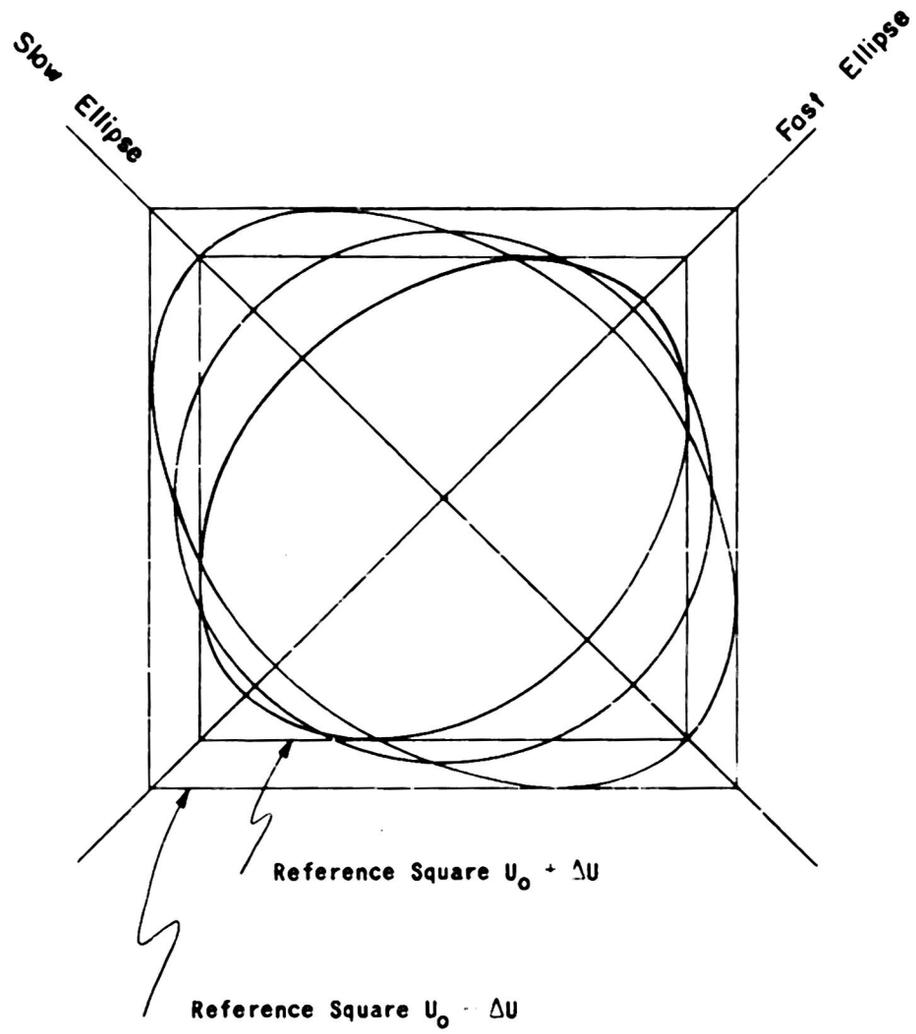


FIGURE F1 BEAM DISPLAY FOR MONOCHROMATIC ELECTRONS HAVING THE VELOCITY $U_0$ (CIRCLE); $U_0 + \Delta U$ (FAST ELLIPSE); $U_0 - \Delta U$ (SLOW ELLIPSE)

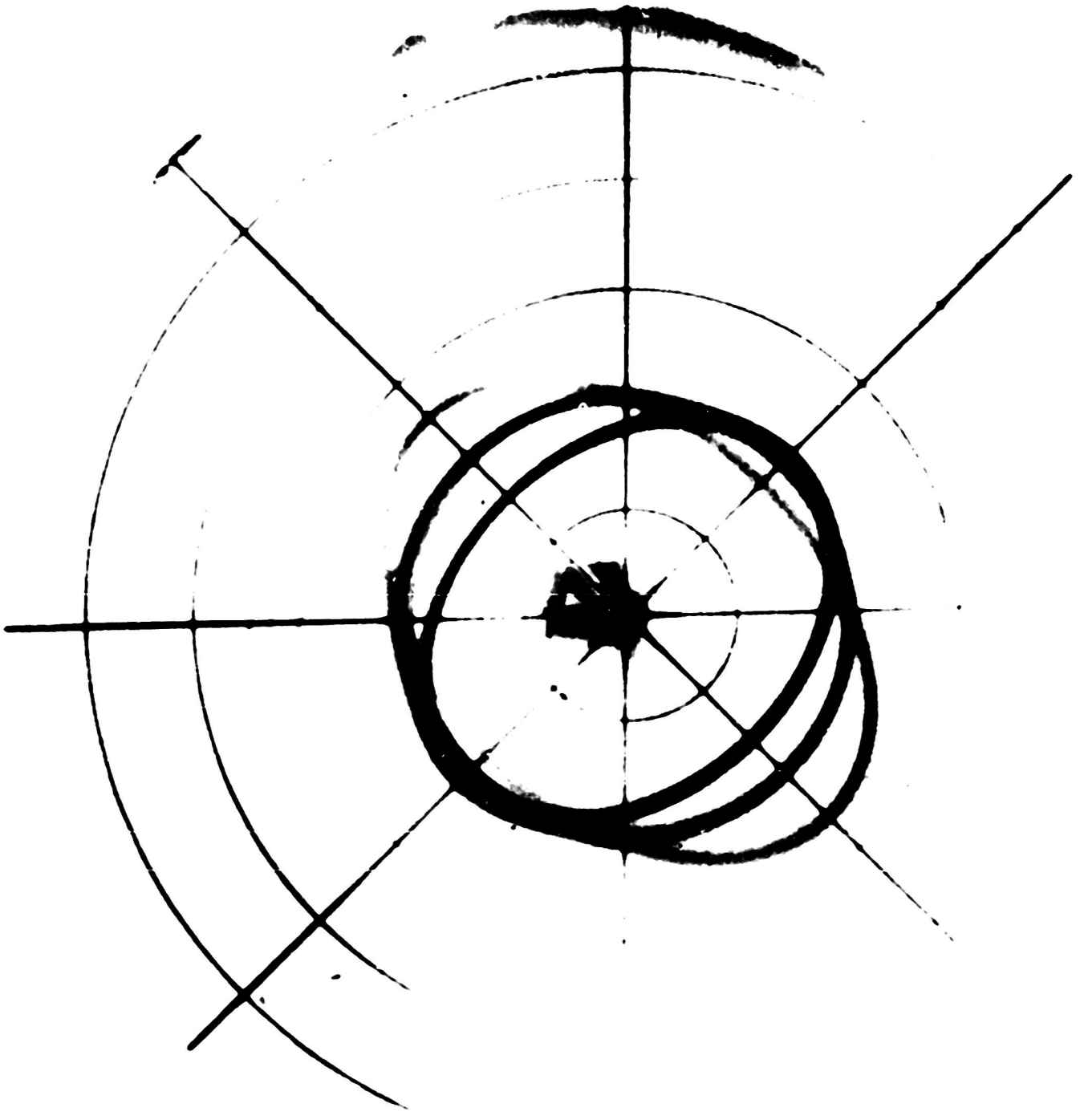

FIGURE B 2 SUPERPOSITION OF THREE MONOCHROMATIC ELECTRON. BEAMS HAVING THE VELOCITIES

$U_0$ = 2000 VOLTS

$U_0 + \Delta U$ = 2300 VOLTS

$U_0 - \Delta U$ = 1700 VOLTS

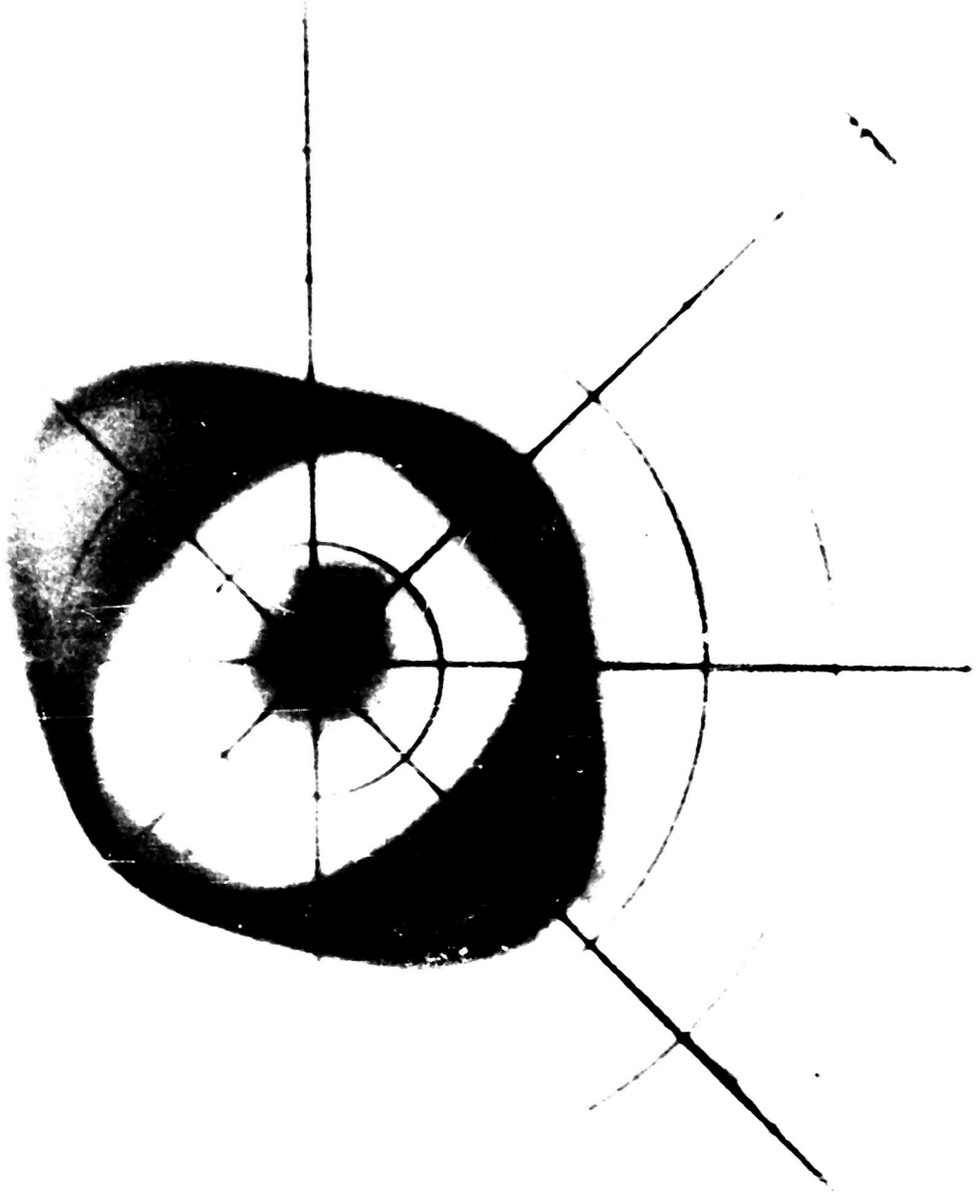

FIGURE 83 POLYCHROMATIC ELECTRON BEAM WITH VELOCITY MODULATION
U = 2000 ± 400 VOLTS
CIRCLE ADJUSTED AT 2000 VOLTS

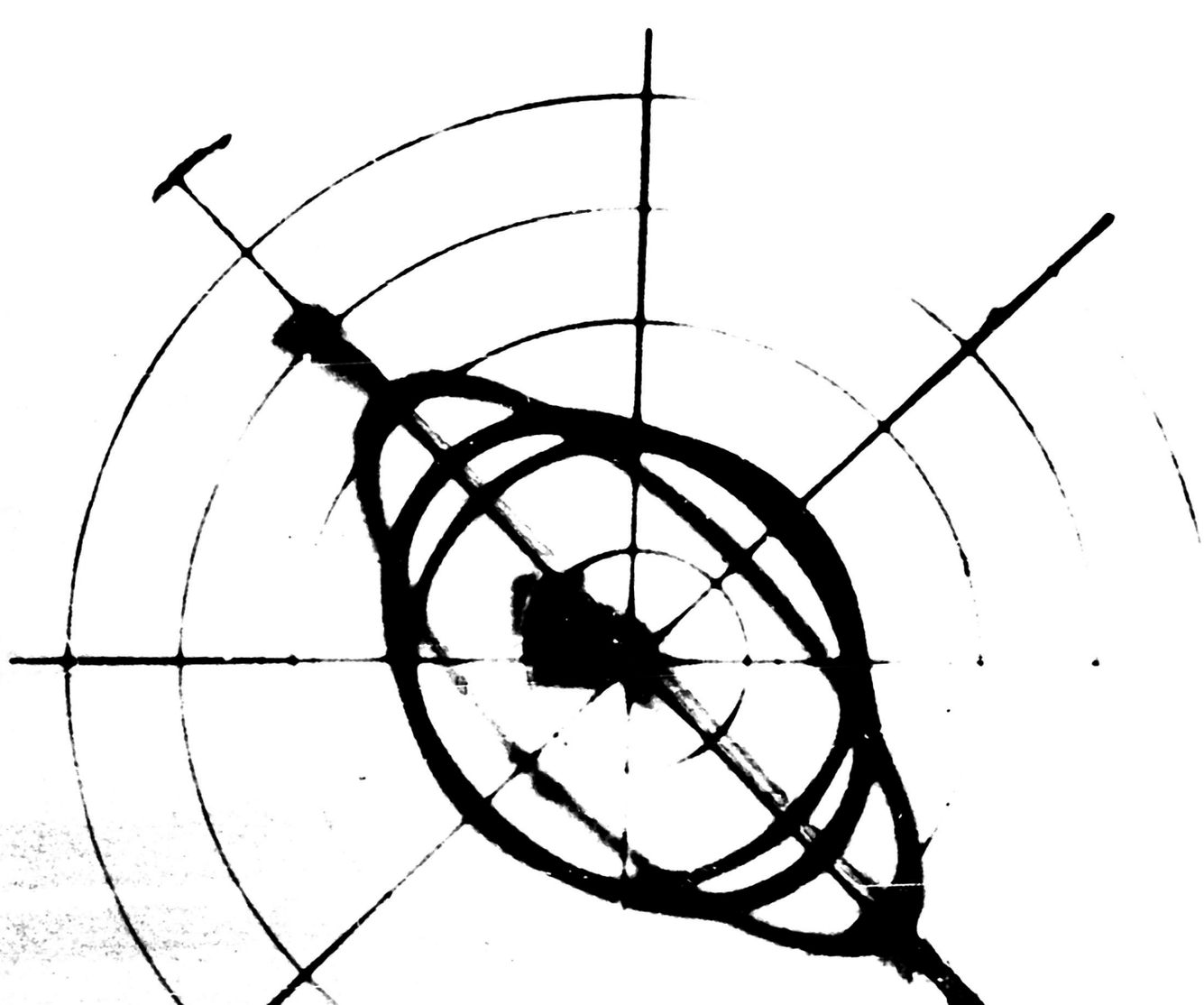

FIGURE B5 SUPERPOSITION OF FOUR MONOCHROMATIC ELECTRON BEAMS HAVING THE VELOCITIES

$U_0$ = 2550 VOLTS (CIRCLE)

$U_1$ = 2250 VOLTS

$U_2$ = 1700 VOLTS

$U_3$ = 1230 VOLTS (LINE)

TOTAL PHASE CHANGE IN THE SYSTEM $\pi/2$

# CHAPTER III

# BEAM ANALYSIS WITH A REMOTE ANALYZER SYSTEM

## SYMBOLS

| | |
|---|---|
| $A$ | a dimension constant |
| $C_h, C_r$ | dimension constants pertaining to h and r expansion |
| $E_h, E_r$ | electric fields in the h and r direction |
| $N$ | number of electrons |
| $dN_\psi, dN_\theta$ | number of electrons pertaining to a phase increment $\psi$ and $\psi + d\psi$ or a deflection increment $\theta$ and $\theta + d\theta$ |
| $I, I_o$ | instantaneous and average electric current |
| $e$ | electron charge |
| $m$ | electron mass |
| $v, v_o, \Delta v$ | electron velocities |
| $k$ | a proportionality constant |
| $s$ | distance of observer and point under observation |
| $h_o, h, h', h''$ | initial height of a disc and its first and second derivatives |
| $r_o, r, r', r''$ | initial radius of a disc and its first and second derivatives |
| $x_o, x, x', x''$ | either $h_o, h, h', h''$ or $r_o, r, r', r''$. |
| $h'_\infty, U_{h\infty}$ | asymptotic velocity in the h direction in cm $sec^{-1}$ and electron volts |
| $r', U_r$ | asymptotic velocity in the r direction in cm $sec^{-1}$ and electron volts |
| $t$ | time |
| $\varphi, \varphi_o$ | driftspace phase angle for electrons having velocities $v, v_o$ |
| $\psi$ | starting phase angle |
| $\varphi$ | arrival phase angle |
| $\varphi_1$ | adjustable phase angle in deflector |

Distribution Functions

| | |
|---|---|
| $M_\psi(\theta)$ | angular distribution function of electrons originating at a starting phase $\psi$ |
| $N_\theta(\psi)$ | phase distribution function of electrons which have accumulated at a deflection angle $\theta$ |
| $m(\theta)$ | density distribution function along the deflection circle |
| $n(\psi)$ | density distribution function along the starting phase |
| $\mu_\psi(\Delta v)$ | velocity distribution function of the $dN_\psi$ electrons pertaining to the phase element $\psi$ |
| $\nu_\theta(\Delta v)$ | velocity distribution function of the $dN_\theta$ electrons pertaining to the angular deflection element $\theta$ |

## 2 DEPHASING OF VELOCITY MODULATED ELECTRONS

Suppose that there are two points along the axis of an RF modulated electron beam, x and x', and that electrons starting with a phase $\psi$ at x, will arrive at the point x' when the analyzer placed at x' is in a phase state $\varphi + \varphi_1$ (see Fig 1) The phase $\varphi_1$ is supposed to be a con-

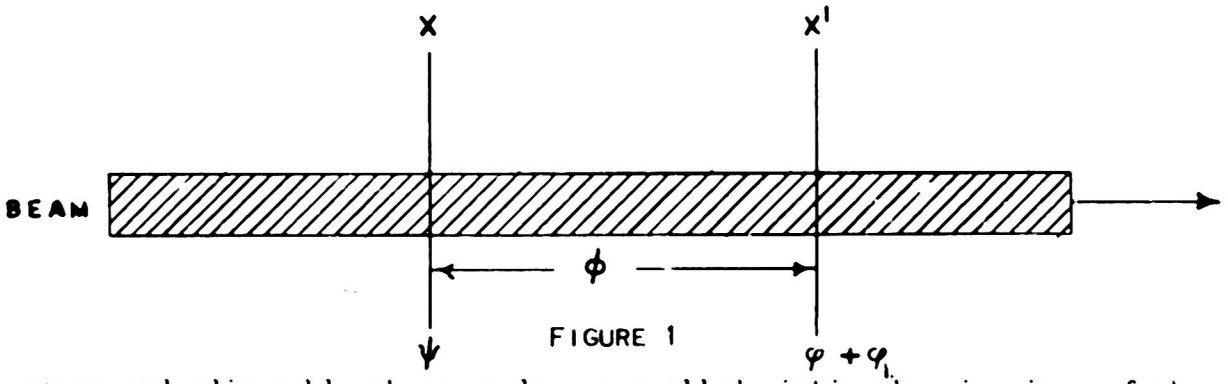


FIGURE 1

stant and adjustable phase angle, controlled within the circuitry of the transmission line Between the starting phase $\psi$ at x and the arriving phase $\varphi$ the following relation can be set up

$$\varphi + \varphi_1 = \phi + \psi \tag{3}$$

where $\phi$ is the phase angle of the drift space between x and x'

$$\phi = 2\pi \frac{x' - x}{\lambda} \frac{c}{v} \tag{4}$$

Defining an average beam velocity $v_o$ and restricting oneself to small velocity deviations $\Delta v$, so that

$$\frac{\Delta v}{v_o} << 1, \tag{5}$$

then the drift space phase angle $\phi$ becomes

$$\phi = 2\pi \frac{x' - x}{\lambda v_o} \left(1 - \frac{\Delta v}{v_o}\right) \tag{6}$$

Introducing

$$\phi_o = 2\pi \frac{S}{\lambda v_o} \tag{7}$$

$$S = x' - x_o \tag{8}$$

Equation (6) changes to

$$\phi = \phi_o - \phi_o \frac{\Delta v}{v_o} \tag{9}$$

Inserting Eq (9) into (3) and adjusting $\varphi_1$ such that $\varphi_1 = \phi_o$, the relation between $\psi$ and $\varphi$ becomes

$$\varphi = \psi - \phi_o \frac{\Delta v}{v_o} \tag{10}$$

This equation permits an important physical interpretation. Suppose the beam under investigation consisted only of extremely sharp bunches following each other at time intervals of one period and starting at x with a phase angle $\psi = 0$ The density function $n(\psi)$ of such a modulated beam is indicated in Fig 2

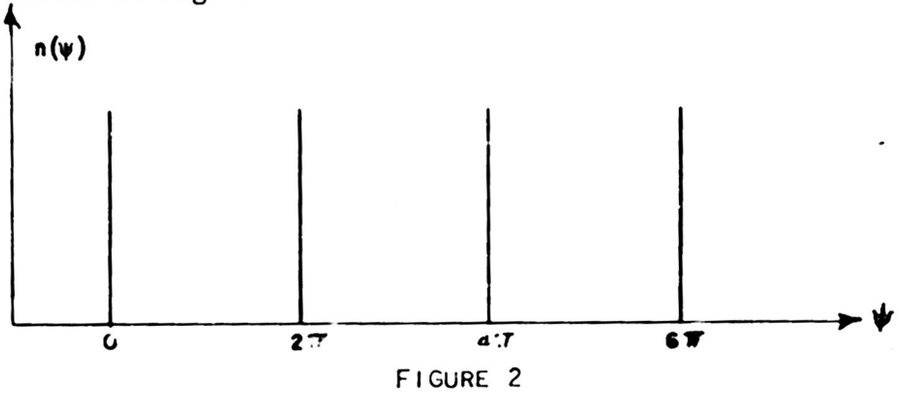


FIGURE 2

Suppose, furthermore, that the electrons in each of these bunches had a velocity spread $\pm\Delta v$ The electrons in this bunch would have spread at x' from $\varphi = -\phi_o \frac{\Delta v}{v_o}$ to $\varphi = +\phi_o \frac{\Delta v}{v_o}$ Since to each phase angle $\varphi$ at the deflector corresponds an angular deflection $\theta$ (see Chapter I), this bunch would appear as a section of a circle, spread over an angle

$$\Delta\theta = 2\phi_o \frac{\Delta v}{v_o} \tag{11}$$

This linear relationship between $\Delta\theta$ and $\Delta v$ can conveniently be used to calibrate a deflection circle directly in terms of velocities, where the velocities can be expressed in electron volts

$$\frac{\Delta v}{v_o} = \frac{1}{2}\frac{\Delta U}{U_o} \tag{12}$$

Equation (11) becomes

$$\Delta\theta^\circ = 1\,8 \times 10^5 \frac{S}{\lambda} U_o^{-3/2} \Delta U \tag{13}$$

For a particular and reasonable example, e g

$$S = 5 \text{ cm}$$

$$\lambda = 10 \text{ cm}$$

$$U_o = 2000 \text{ volt}$$

Eq. (13) reduces to

$$\Delta\theta^\circ \quad \Delta U/\text{volts}$$

and the deflection circle can easily be calibrated (see Fig. 3)

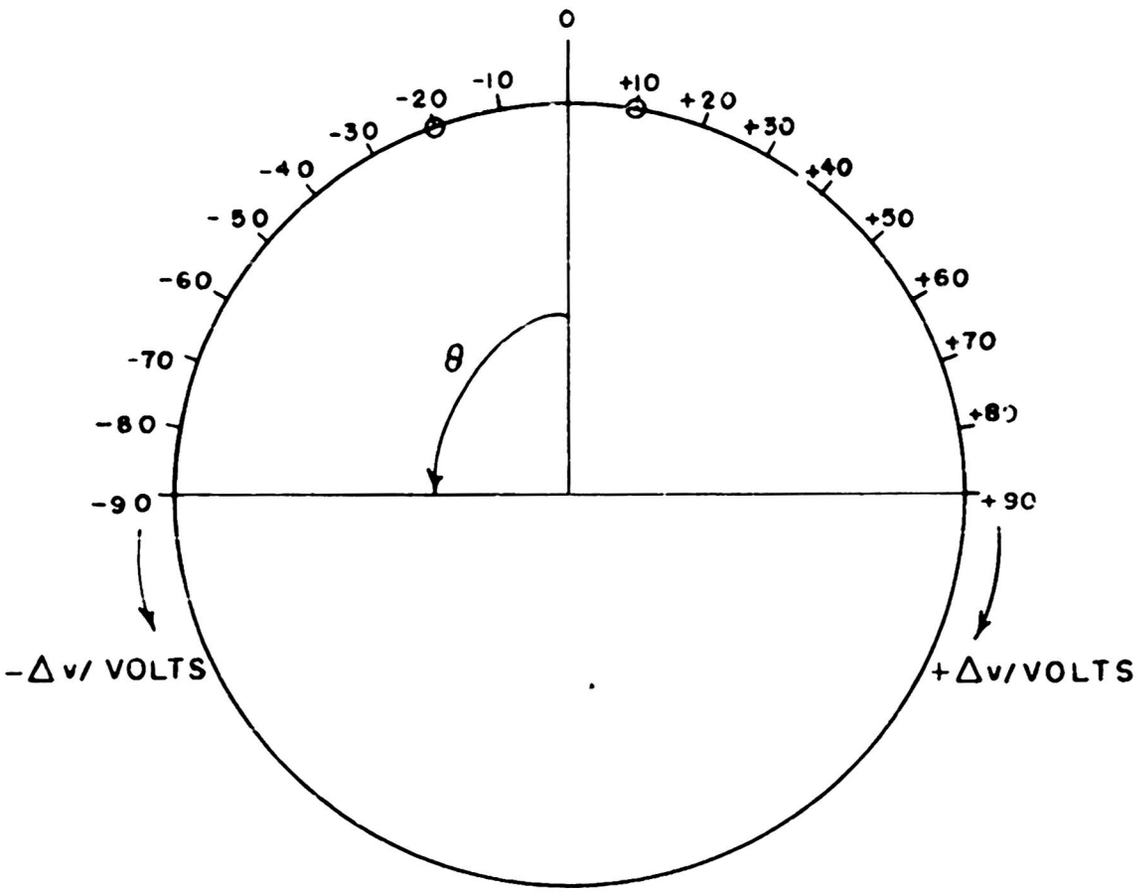


FIGURE 3

The interpretation of this figure is simple. Assume two electrons passing the point x at $\psi = 0$ and having velocities 2010 and 1980 volts. They will project themselves on the circle at the points +10 and -20. This technique can be used to construct a very accurate velocity analyzer. In this context, however, the phenomenon qualifies itself as an aberration.

In this particular example a very specialized beam type was assumed. A beam consisting of a series of infinitesimally small bunches is a desirable feature, but unfortunately a rare exception. For usual cases a more general treatment seems therefore necessary. Sufficient generality is guaranteed by assuming the beam at the point x is periodically modulated with an arbitrary density function $n(\psi)$. Within a phase element $\psi$ and $\psi + d\psi$ there will be dN electrons defined according to Eq. (2)

$$dN_\psi = n(\psi)d\psi \tag{14}$$

The index x in Eq. (2) can be omitted, for only this point will be considered.

The question now arises as to what way this velocity distribution function will map itself on the observation plane In other words, what will the angular distribution function look like, if the velocity distribution is given? Since the angular deflection angle $\theta$ is identical to the phase angle $\varphi$ at the point x', either $\theta$ or $\varphi$ can be used to define such a distribution function Let us choose $\theta$; then an angular distribution function

$$M_\psi(\theta) = \left( \frac{d(dN)}{d\theta} \right)_\psi \tag{16}$$

can be defined which describes the distribution of those electrons along the deflection circle, which originates from a starting phase $\psi$ (See Fig 6 ) It is now necessary to transform the $\mu$-function into the

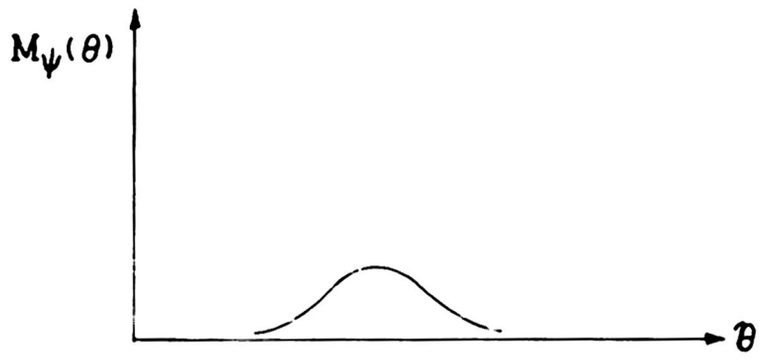


FIGURE 6

M-function. The link to this transformation is Eq (10) which correlates $\varphi$, $\psi$ and v Using the identity

$$\varphi \equiv \theta, \tag{17}$$

then

$$\theta = \psi - \phi_o \frac{\Delta v}{v_o} \tag{18}$$

Differentiating $\theta$ with respect to $\Delta v$ and keeping $\psi$ constant correlates the angular increment $d\theta$ with the velocity increment $d\Delta v$. One obtains

$$d\theta = - \frac{\phi_o}{v_o} d\Delta v \tag{19}$$

Dividing this equation by ddN and inverting it, one gets

$$\frac{d(dN)}{d\theta} = - \frac{v_o}{\phi_o} \frac{d(dN)}{d(\Delta v)} \tag{20}$$

Using the definitions for $\mu$ and M from Eqs (15) and (16), Eq. (20) becomes

$$M_\psi(\theta) = - \frac{v_o}{\phi_o} \mu_\psi(\Delta v) \tag{21}$$

The transformation would be completed if the argument in both functions were the same. Using again Eq (18) to express $\Delta v$ in terms of $\theta$

$$\Delta v = \frac{v_o}{\phi_o} (\psi - \theta) \tag{22}$$

and introducing this in (21), the transformation is completed and reads

$$M_{\psi_1}(6) = - \frac{v_o}{\phi_o} \mu_{\psi_1} \left( \frac{v_o}{\phi_o} (\psi_1 - \theta) \right) \tag{23}$$

The index 1 in $\psi$ indicates that this is the angular distribution of electrons originating from a particular phase angle $\psi_1$. It is interesting to note that the original distribution function $\mu$ is completely preserved in its form; only the x and y coordinates are stretched with the factor $v_o/\phi_o$ to compensate for the change of dimensions, and the whole function is shifted along the $\theta$ axis with the amount $\psi_1$

Equation (23) immediately gives an answer to the question How many electrons from an arbitrary starting phase $\psi$ are contributed to a particular deflection angle $\theta$? The answer is

$$M_{\psi}(\theta_1) = - \frac{v_o}{\phi_o} \mu_{\psi} \left( \frac{v_o}{\phi_o} (\psi - \theta_1) \right) \tag{24}$$

To know how many electrons from all phases $\psi$ are contributed to a particular deflection angle $\theta$, one has only to integrate over the M-function

$$m(\theta) = \int_{-\infty}^{\theta} M_{\psi}(\theta)\, d\psi = - \frac{v_o}{\phi_o} \int_{-\infty}^{\theta} \mu_{\psi} \left( \frac{v_o}{\phi_o} (\psi - \theta) \right) d\psi \tag{25}$$

In this m-function one meets the counterpart of the originally introduced n-function. If $n(\psi)$ is the density distribution function of the electrons along the starting phase $\psi$, the function $m(\theta)$ gives the density distribution function of the electrons along the circle. The m-function is that which one observes. $m(\theta)$ is the number dN of electrons arriving within a deflection angle increment $\theta$ and $\theta + d\theta$ on the observation plane (see Fig. 7)

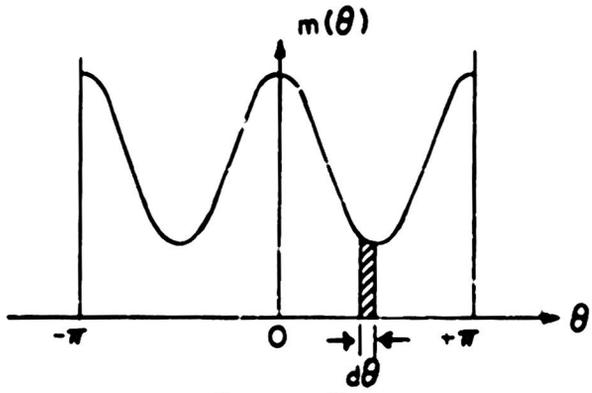


FIGURE 7

Using a small angular aperture (Fig 8), $m(\theta)$ can easily be measured by measuring the current passing that aperture From this bit of

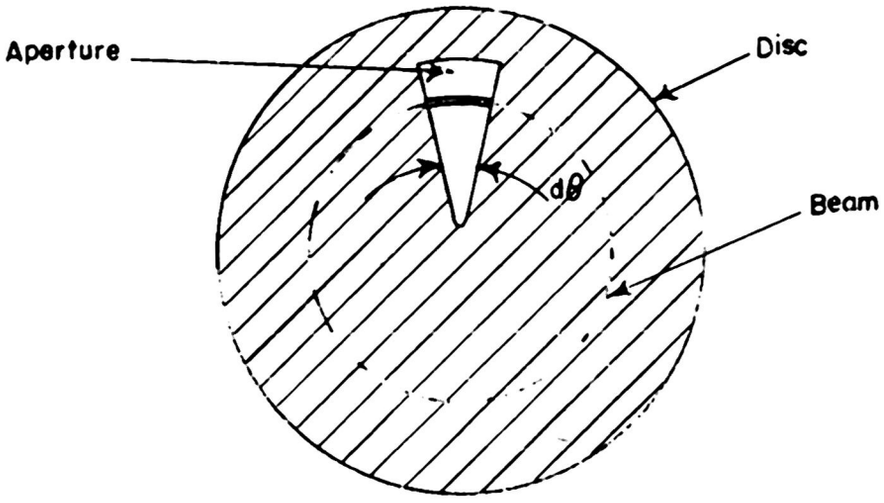


FIGURE 8

information it is possible in principle to recalculate the original density distribution $n(\psi)$ and the velocity distribution functions $\mu_\psi$ if the factor $v_o/\phi_o$ can be varied That is always the case because $v_o/\phi_o$ contains only the beam voltage and the distance $x - x$ Since this technique encounters some mathematical complications which would go beyond this elementary treatment, it will be reported separately elsewhere

Instead another approach will be used here to trace back the original beam properties The method consists of a velocity analysis of each arriving phase increment $\varphi$ and $\varphi + d\varphi$ (or $\theta$ and $\theta + d\theta$) In the beam analyzer built in this laboratory this means is provided (See Progress Report XIX-14 )

Suppose that with such an angular aperture a function

$$m(\theta) = \frac{dN}{d\theta} \tag{26}$$

could be measured Then corresponding to each angular increment $d\theta$ there will be dN electrons, defined according to Eq (26) as

$$dN_\theta = m(\theta)d\theta \tag{27}$$

The index $\theta$ in dN makes sure that these electrons belong to the deflection angle $\theta$ Now, suppose that for these $dN_\theta$ electrons pertaining to a deflection angle $\theta$ a particular velocity distribution function $v_\theta(\Delta v)$ has been found $v_\theta(\Delta v)$ is defined as

$$v_\theta(\Delta v) = \left( \frac{ddN}{d\Delta v} \right)_\theta \tag{28}$$

(See Fig 9 )

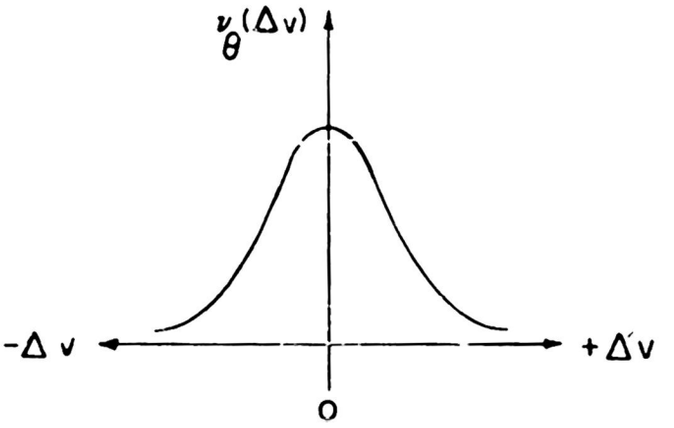


FIGURE 9

The question now arises as to what way this velocity distribution function will map itself back at the starting point x. In other words, how were those electrons distributed along the entrance phase $\varphi$ to arrive simultaneously at the phase $\Phi$ (or $\theta$) with that measured velocity distribution? Let us define a phase-distribution function

$$N_\theta(\psi) = \left(\frac{ddN}{d\psi}\right)_\theta \tag{29}$$

which describes the distribution of those electrons along the starting phase $\psi$, which later accumulated at the phase angle $\theta$

To transform the v-function into the N-function Eq (18) will be used again to establish a relation between $\psi$, $\theta$ and $\Delta v$ Properly rearranged (18) reads

$$\psi - \theta + \phi_o \frac{\Delta v}{v_o} \tag{30}$$

Differentiating $\psi$ with respect to $\Delta v$, keeping $\theta$ constant, correlates the phase increment $d\psi$ with the velocity increment $\Delta v$

$$d\psi = \frac{\phi_o}{v_o} d\Delta v \tag{31}$$

Proceeding in a manner analogous to the considerations condensed in Eqs (20) to (23) (see page 64) one obtains the transformation $v \rightarrow N$ in the following form

$$N_{\theta_1}(\psi) = \frac{v_o}{\phi_o} v_{\theta_1}\left(\frac{v_o}{\phi_o}(\psi - \theta_1)\right) \tag{32}$$

The index 1 in $\theta$ indicates that this is the phase distribution of electrons along $\psi$, later accumulating at a particular deflection angle $\theta_1$

Following precisely the strategy applied to the distribution function M, one can easily determine how many electrons from an arbitrary deflection angle $\theta$ have originated in a particular phase angle $\psi_1$. The answer is

$$N_\theta(\psi_1) = \frac{v_o}{\phi_o} \nu_\theta \left( \frac{v_o}{\phi_o}(\psi_1 - \theta) \right) \tag{33}$$

Finally the original distribution function $n(\psi)$ can be found by adding all the electrons which started at $\psi$ and arrived at all possible deflection angles $\theta$. Thus

$$n(\psi) = \int_o^{2\pi} N_\theta(\psi)\ \theta = \frac{v_o}{\phi_o} \int_o^{2\pi} \nu_\theta\left( \frac{v_o}{\phi_o}(\psi - \theta) \right) d\theta. \tag{34}$$

Since $\nu_\theta$ can be measured for all deflection angles $\theta$, the integration (34) can be carried out graphically or numerically.

With Eq. (34) the question of this section is answered: how to correct angular aberrations which are caused by an undesired drift space between the point of interest and the point of analysis by presence of a finite velocity distribution of the electrons in the beam.

## 3. DEBUNCHING EFFECTS

In this section a rough estimate of the amount of velocity modulation and increase of linear extension of a beam section will be made, assuming that a tight bunch of N electrons all having the same velocity $v_o$ will pass through the point of interest x, but will be observed at a later point x'. Since in the meantime electrostatic forces will be at work to debunch the bundle, a velocity component may be superimposed at the point x' which was originally non-existent; this will increase the length of the original bunch.

Suppose the original bunch is a short cylinder with the following geometrical properties: Height $h_o$ and base circle radius $r_o$. See Fig. 10.

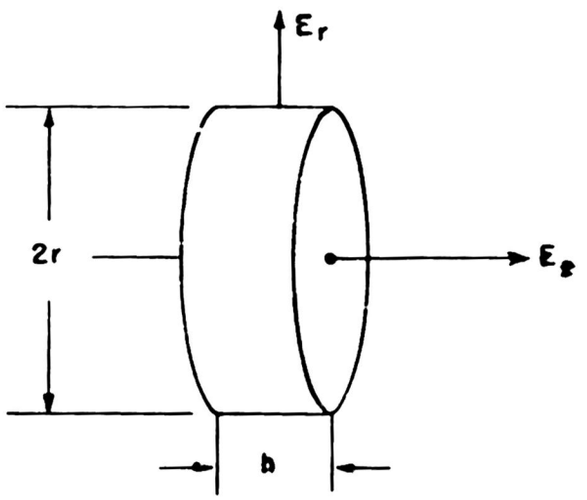


FIGURE 10

During its expansion its dimension may be h and r. The expressions for the fields in the z and r direction can be approximately determined assuming the disc to be very flat. Then

$$E_z = 2\pi\rho h \tag{35}$$

$$E_r = 2\pi\rho r \tag{36}$$

Suppose the disc contains N electrons; then the space charge $\rho$ becomes

$$\rho = \frac{eN}{\pi r^2 h} \tag{37}$$

Setting up the equation of motion in both directions

$$h'' = \frac{d^2h}{dt^2} = \frac{e}{m} E_z \tag{38}$$

$$r'' = \frac{d^2r}{dt^2} = \frac{e}{m} E_r \tag{39}$$

and inserting into (35) and (36) the expressions for $\rho$, one obtains

$$\frac{d^2h}{dt^2} = \frac{2e^2N}{m}\frac{1}{r^2} \tag{40}$$

$$\frac{d^2r}{dt^2} = \frac{2e^2N}{m}\frac{1}{rh} \tag{41}$$

These two differential equations have to be solved simultaneously, since each one contains the argument of the other one.

Defining a constant

$$A = \frac{2e^2N}{m}, \tag{42}$$

the above equations become

$$h'' = A\frac{1}{r^2} \tag{43}$$

$$h'' = A\frac{1}{rh} \tag{44}$$

Proving first that the assumption

$$r = kh \tag{45}$$

is correct, where k is a constant and is defined by the initial condition

$$r_o = kh_o, \tag{46}$$

because from (45) one gets

$$r'' = kh''$$

which is true as one immediately sees by dividing (43) into (44), the mathematical problem is reduced to finding solutions for the two differential equations:

$$h'' = \frac{A}{k^2}\cdot\frac{1}{h^2} \tag{47}$$

$$r'' = Ak\frac{1}{r^2} \tag{48}$$

Both equations are of the same type, viz,

$$x'' = C\frac{1}{x^2} \tag{49}$$

where only the constants differ in the two cases.

$$C_h = A\frac{h_o^2}{r_o^2} \tag{50}$$

$$C_r = A\frac{r_o}{h_o} \tag{51}$$

Solutions for the differential equation (49) are readily obtained. With the initial conditions

$$\text{for} \quad t = 0 \qquad \begin{cases} x' = 0 \\ x = x_c, \end{cases} \tag{52}$$

the first integral becomes

$$x' = \sqrt{\frac{2C}{x_o}} \sqrt{1 - \frac{x_o}{x}} \tag{53}$$

and the second

$$x = x_o F\left(\frac{t}{t_o}\right) \tag{54}$$

whereby the function F is defined as

$$F(\cosh^{-1}\sqrt{z} + \sqrt{z}\sqrt{z-1}) = z \tag{55}$$

and is plotted in Fig. (11).

The time constant, $t_o$, is

$$t_o = \sqrt{\frac{x_o^3}{2C}} \tag{56}$$

Evaluating this formula for both cases, r and h, one obtains with (50) and (51)

$$t_o = t_{oh} = t_{or} = \sqrt{\frac{r_o^2 h_o}{2A}} \tag{57}$$

The solutions for h and r are finally

$$\left.\begin{aligned} \frac{h'}{h_o} &= \frac{1}{t_o}\sqrt{1 - \frac{h_o}{h}} \\ \frac{r'}{r_o} &= \frac{1}{t_o}\sqrt{1 - \frac{r_o}{r}} \end{aligned}\right\} \tag{58}$$

$$\frac{h}{h_o} = \frac{r}{r_o} = F\left(\frac{t}{t_o}\right) \tag{59}$$

Two features of the above equations are worthwhile to note:

a) The time constant of expansion in both directions is the same.
b) The velocity of expansion reaches an asymptotic value in both cases, because for h or r approaching infinity one obtains

$$h'_\infty = \sqrt{\frac{2Ah_o}{r_o^2}} \quad (60) \qquad r'_\infty = \sqrt{\frac{2A}{h_o}} \quad (61)$$

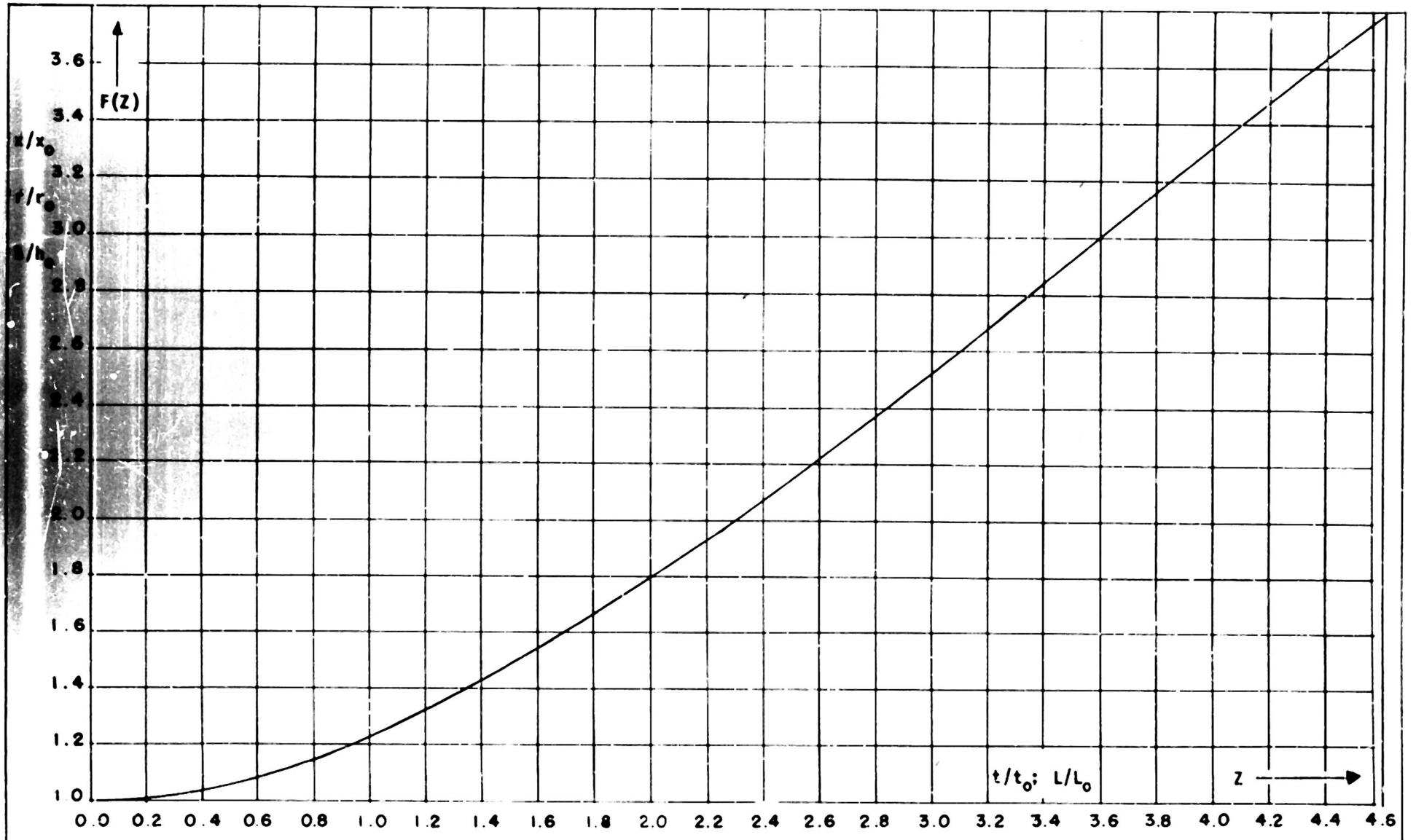
F(Z)
3.6
3.4
3.2
3.0
2.8
2.6
2.4
2.2
2.0
1.8
1.6
1.4
1.2
1.0
0.0 0.2 0.4 0.6 0.8 1.0 1.2 1.4 1.6 1.8 2.0 2.2 2.4 2.6 2.8 3.0 3.2 3.4 3.6 3.8 4.0 4.2 4.4 4.6
t/t0; L/L0
Z

FIGURE 11

To arrive at more convenient units the constant A will be computed from Eq. (42). Introducing an average current per period T

$$I_o = \frac{\int_0^T I dt}{T} \tag{62}$$

with

$$I = e \frac{dN}{dt}$$

$$\int dN = N$$

$$T = \frac{\lambda}{c}$$

one obtains for (62)

$$I_o = eN \frac{c}{\lambda} \tag{63}$$

With this, A becomes

$$A = \frac{2eI_o}{m} \frac{\lambda}{c} \tag{64}$$

The asymptotic values for the velocities in the x and r direction expressed in electron volts finally become

$$U_{r_\infty} = 60 \frac{\lambda}{h_o} I_o/\text{Amp.} \tag{65}$$

$$U_{h_\infty} = 60 \frac{h_o \lambda}{r_o^2} I_o/\text{Amp.} \tag{66}$$

These values represent upper limits of the velocity to which electrons can be accelerated if they originally belonged to a tight bunch with the dimension $h_o$ and $r_o$. If these velocities turn out to be very small in comparison with the beam voltage, then one can forget about them. However, if they do not turn out to be negligible, one can expect aberrations unless one decreases one decisive parameter, viz, the current, by choosing a smaller aperture.

To get also a better feeling for the magnitude of the expansion process it is convenient to ask to what extent, $x/x_o$, of its original dimension the bunch will expand after it has traveled a particular distance L. Calling the velocity of the bunch $v_o$, then

$$L = v_o t \qquad \text{and} \quad L_o = v_o t_o.$$

Equation (59) becomes

$$\frac{x}{x_o} = F\left(\frac{L}{L_o}\right) \tag{67}$$

# Distribution List for Technical Reports
## N6-ori-71 Task XIX
## NR 073 162

Copies

2 Office of Naval Research (427)
Navy Department
Washington 25, D. C.

9 Naval Research Laboratory
Technical Information Officer
Attn: Code 2027
Washington 20, D. C.

6 Library of Congress
Navy Research Section
Washington 25, D. C.

1 Commanding Officer
U. S. Navy, Office of Naval Research
Branch Office
801 Donahue Street
San Francisco 24, California

1 Commanding Officer
U. S. Navy, Office of Naval Research
Branch Office
Navy 100, Fleet Post Office
New York, N. Y.

1 Commanding Officer
U. S. Navy, Office of Naval Research
Branch Office
1030 E. Green Street
Pasadena 1, California

1 Commanding Officer
U. S. Navy, Office of Naval Research
Branch Office
495 Summer Street
Boston 10, Massachusetts

2 Commanding Officer
U. S. Navy, Office of Naval Research
Branch Office
America Fore Building
844 North Rush Street
Chicago 11, Illinois

Copies

1 Commanding Officer
U. S. Navy, Office of Naval Research
Branch Office
346 Broadway
New York 13, N. Y.

1 Director
Naval Ordnance Laboratory
White Oak, Maryland

2 Chief, Bureau of Ships (810)
Navy Department
Washington 25, D. C.

1 Chief, Bureau of Ships (836)
Navy Department
Washington 25, D. C.

1 Chief, Bureau of Aeronautics (EL-4)
Navy Department
Washington 25, D. C.

1 Chief, Bureau of Aeronautics (EL-54)
Navy Department
Washington 25, D. C.

1 Chief, Bureau of Aeronautics (EL-91)
Navy Department
Washington 25, D. C.

1 Chief, Bureau of Ordance (Re 4)
Navy Department
Washington 25, D. C.

1 Chief, Bureau of Ordance (Re 9)
Navy Department
Washington 25, D. C.

1 Chief of Naval Operations (Op-20)
Navy Department
Washington 25, D. C.

Copies

1 Chief of Naval Operations (Op 413)
Navy Department
Washington 25, D. C.

1 U. S. Naval Proving Ground
Dahlgren, Virginia
Attn: W. H. Benson

1 Director
Naval Electronics Laboratory
San Diego 52, California

1 Naval Research Laboratory (3470)
Washington 20, D. C.

1 U. S. Naval Academy
Post Graduate School
Electrical Engineering Department
Annapolis, Maryland

1 U. S. Coast Guard (EEE)
1300 E Street, N. W.
Washington 25, D. C.

3 Commanding Officer
Signal Corps Engineering Laboratories
Evans Signal Laboratory
Belmar, New Jersey
Attn: Chief, Thermionics Branch

1 Research and Development Board
Pentagon Building
Washington 25, D. C.

1 Panel on Electron Tubes
Research and Development Board
139 Centre Street, Room 601
New York 13, N. Y.

1 Massachusetts Institute of Technology
Research Laboratory of Electronics
Cambridge 39, Massachusetts
Attn: Professor A. G. Hill

1 Massachusetts Institute of Technology
Laboratory for Insulation Research
Cambridge 39, Massachusetts
Attn: Professor A. von Hippel

Copies

1 Harvard University
Cruft Laboratory
Cambridge, Massachusetts
Attn: Professor E. L. Chaffee

1 Yale University
Dunham Laboratory
New Haven, Connecticut
Attn: Professor H. J. Reich

1 Yale University
Sloane Physics Laboratory
New Haven, Connecticut
Attn: Professor Robert Beringer

2 Commanding General
Air Materiel Command
Electronics Subdivision
Wright-Patterson Air Forces Base
Dayton, Ohio
Attn: MCREE3-33

2 Commanding Officer
Watson Laboratories
Red Bank, New Jersey
Attn: Mr. O. R. Lovitt WLECP-1B

2 Commanding Officer
Cambridge Field Service
230 Albany Street
Cambridge 39, Massachusetts
Attn: Dr. L. M. Hollingsworth

1 Polytechnic Institute of Brooklyn
Microwave Research Institute
55 Johnson Street
Brooklyn 1, N. Y.
Attn: Professor Ernst Weber

1 Princeton University
Electrical Engineering Department
Princeton, N. J.
Attn: Professor C. H. Willis

1 University of California
Electrical Engineering Department
Berkeley 4, California
Attn: Professor T. C. MacFarland

Copies

1 Raytheon Manufacturing Company
Waltham, Massachusetts
Attn: H. R. Argento

1 Airborne Instruments Laboratory
160 Old Country Road
Mineola, L. I., N. Y.
Attn: Mr. John Byrne

1 Sperry Gyroscope Company
Great Neck, Long Island
New York
Attn: Robert L. Wathen

1 Dr. E. L. Ginzton
Microwave Laboratory
Physics Department
Stanford University
Stanford, California

1 Dean F. E. Terman
School of Engineering
Stanford University
Stanford, California

1 Electronics Research Laboratory
Department of Electrical Engineering
Stanford University
Stanford, California
Attn: Professor Karl Spangenberg

Copies

1 General Electric Company
Research Division
Schenectady, New York
Attn: Mr. E. D. McArthur

1 University of Washington
Electrical Engineering Department
Seattle, Washington
Attn: Professor A. E. Harrison

1 British Joint Services Mission
(Technical Services)
P. O. Box 680
Benjamin Franklin Station
Washington, D. C.

1 British Commonwealth Scientific Office
1785 Massachusetts Avenue, N. W.
Washington, D. C.

1 Dr. J. R. Pierce
Bell Telephone Laboratories
Murray Hill, New Jersey